DEVELOPMENT OF A SMART SYSTEM FOR LEAK DETECTION IN WATER DISTRIBUTION NETWORKS

by

Doha Hesham Elshazly

A Thesis presented to the faculty of the
American University of Sharjah
College of Engineering
In Partial Fulfillment
of the Requirements
for the Degree of

Master of Science in
Civil Engineering

Sharjah, United Arab Emirates

December 2021

Declaration of Authorship

I declare that this thesis is my own work and, to the best of my knowledge and belief, it does not contain material published or written by a third party, except where permission has been obtained and/or appropriately cited through full and accurate referencing.

Signed 

Date 21/11/2021

Approval Signatures

We, the undersigned, approve the Master's Thesis of Doha Hesham Elshazly

Project Title: Development of a Smart System for Leak Detection in Water Distribution Networks

Data of Defense: 21/11/2021

Name, Title and Affiliation **Signature**

Dr. Tarig A. Ali
Professor, Department of Civil Engineering
Thesis Advisor

Dr. Md. Mortula
Professor, Department of Civil Engineering
Thesis Co-Advisor

Dr. Serter Atabay
Professor, Department of Civil Engineering
Thesis Committee Member

Dr. Lutfi Albasha
Professor, Department of Electrical Engineering
Thesis Committee Member

Dr. Irtishad Ahmad
Head, Department of Civil Engineering

Dr. Lotfi Romdhane
Associate Dean for Graduate Affairs and Research
College of Engineering

Dr. Sameer Al-Asheh
Interim Dean
College of Engineering

Dr. Mohamed El-Tarhuni
Vice Provost for Research and Graduate Studies

Acknowledgement

I would like to convey my warmest thanks to my advisors Dr. Tarig Ali and Dr. Md. Mortula for providing me with knowledge, guidance, support, and encouragement during all stages of my project. I owe them a debt of gratitude for their invaluable support, thoughtful discussion, and helpful suggestions.

I would like to express my gratitude to the instructors of the Civil Engineering department who taught me the master's level courses using effective teaching methods and techniques. I am grateful for their wise counsel and encouragement. Additionally, I am thankful for getting the opportunity to work as a graduate teaching assistant at the American University of Sharjah.

I would also like to thank the committee members for making my defense a pleasant experience and for your insightful remarks and ideas, which helped me further improve my thesis quality.

Dedication

I dedicate my thesis to my family and friends. A heartfelt gratitude to my devoted parents, whose words of encouragement and insistence on perseverance still ring in my ears. I would also like to thank my sisters who have never left my side and are very special to me.

I also dedicate this work to my many friends who have supported me along the way. I will always appreciate everything they have done.

Abstract

Water is a critical source of life for the human society, which needs to be sustained. Every year, a considerable portion of water is lost from water distribution networks (WDNs) due to leaks. This is accompanied by significant consequences including, economic losses and supply disruption, which are major concerns for water utility companies. Hence, a robust and timely leak detection method is necessary to conduct corrective maintenance so as to minimize the underlying consequences. Previous studies have investigated the efficiency and effectiveness of various nondestructive detection methods including ground penetrating radar (GPR), spectrometry, and infrared sensing. Based on the outcome of the recent research on leak detection using infrared sensing, this study aims to develop a smart leak detection system that integrates remote sensing and geographic information system (GIS). The proposed system is to be used by a drone, equipped with an infrared (IR) camera, and geospatial analysis tools that incorporate remote sensing and GIS for near-real time leak detection. In addition, this study utilizes currently installed pressure, flow and water quality monitoring sensors in WDNs. A GIS customized interface was developed to automate the leak detection system and allow for timely data processing. The proposed system was validated on a section of the WDN in the city of Sharjah, in collaboration with Sharjah Electricity and Water Authority (SEWA). The results obtained in this research proved the efficiency of the proposed method for leak detection in WDNs.

Keywords: GIS, leak detection, infrared thermography, automation, drone.

Table of Contents

List of Figures

List of Tables

List of Abbreviations

GIS	Geographic Information System
GPS	Global Positioning System
GPR	Ground Penetrating Radar
IDW	Inverse Distance Weighting
ISDW	Inverse Square Distance Weighting
IR	Infrared
SEWA	Sharjah Electricity and Water Authority
WDN	Water Distribution Network

Chapter 1. Introduction

Water is a key element in the human society, not solely for drinking, but it is an essential component of all forms of social and economic development and a fundamental element in several nature's processes [1]. The concurrent rapid pace of urbanization yields increased water demand, which imposes a challenge on the water utilities to supply adequate water of sufficient quality. However, lack of water resources is an impeding issue, since only 2.5 % of the available water on earth is fresh water. Majority of the fresh water is often found in inaccessible areas including deep aquifers and glaciers [2]. Therefore, other alternative water sources such as surface and desalinated water are often treated and delivered to consumers. Water utilities deliver treated water to consumers through supply systems (WDNs). There are different types of water supply systems including dead end or tree system, gridiron system, circular or ring system and radial system. Dead end or tree system consists of a single main pipeline lying along the length of a populated area with sub-mains leading to branches to the houses. Similarly, the gridiron system comprises a main pipe with perpendicular sub-mains and branches interconnecting them. Circular or ring systems include pipes forming a loop surrounding a distribution area. Radial systems sub divides an area such that each sector contains a centered reservoir from which pipes run radially to their destination. The purpose of WDNs is to deliver adequate clean water to the consumers, which is often unmet due to potential deficiencies in network. According to Hunaidi et al. (1999) around 25% of the water produced is lost during the distribution process every year as a result of theft, leakage or metering errors, among which leakage is the main contributor [3]. Water loss from old pipes can go up to 50%, exhausting valuable natural resources as well as causing economic losses [3]. The financial losses include the cost of raw water extraction, its treatment and delivery. Additionally, leaks cause pipe deterioration in the form of erosion and pipe breakage, which can damage roads and building foundations.

Numerous studies have explored issues related to water leakage in WDNs and several leak detection techniques have been tested. The most commonly used practices include acoustic equipment, infrared thermography, pressure and flow sensor sensors, and GPRs [4],[5]. These methods have been efficiently implemented for decades to detect leaks, owing to their cost effectiveness and practicality. However, some of these

methods showed limited success due to certain uncertainties, inaccuracies, and its limited applicability on a laboratory setting. Limitations range from efficiency to the need for skilled labors on site. Although acoustic techniques are cost effective, low accuracy in noisy situations, loss of time information, and absence of mathematical reliability (the consistency of the instrument measurements) remain unsolved issues. In addition, it is a slow process that requires experienced human intervention [6],[7]. Relying solely on pressure-based technologies was proven inaccurate due to the interference of other factors affecting pressure readings apart from leakage. In addition, localizing the sensors through the network to improve the accuracy of the results requires optimization, which can be challenging for large WDNs [8]. Although GPR works flexibly for all pipe sizes and materials, it is occasionally inefficient in detecting the exact leak location [9],[10]. Lastly, infrared thermography can provide inaccurate results when relied on solely for leak detection as it can detect other environmental conditions (e.g., shadows) as leaks.

1.1 Problem Statement

Potable water is a critical source of life for the human society, which needs to be sustained. A considerable portion of water is lost in water distribution networks (WDNs) due to leaks. Failure in the delivery process can lead to financial complications and health problems as pressure in the pipe system drops. Additionally, leaks within the network can lead to environmental complications, because of the massive waste of energy. Water losses due to leaks account for 30% of the total water produced and can reach 50% in older pipes [3]. Major causes of pipe leakage include poor WDN maintenance, sudden changes in water pressure, or due to corrosion, cracks and defects in the pipes. Those leaks cause a threat as they exhaust a valuable natural resource and money. The primary economic loss comes from the extraction of raw water, its treatment, and transportation in the WDN. Leakage inevitably also results in secondary economic losses in the form of damage to the pipe network itself and damage to foundations of roads and buildings. Leaky pipes can also cause public health risk because leaks are a potential entry point for contaminants from the soil, as it causes pressure drops in the WDN. Therefore, leakage has been a major concern for the water utility authorities.

1.2 Research Objectives

This research aims at developing a smart leak detection system that uses remote sensing and GIS techniques. Specifically, the research objectives are: 1) identify potential leak locations using pressure, flow and water quality information obtained from water utility companies, based on GIS techniques. 2) identify exact leak locations by acquiring IR images for the identified potential leak areas. 3) develop a GIS customized interface that facilitates the automation of the leak detection process. However, due to the pandemic restrictions, the second step was replaced by a lab-scale setup of a WDN, which served as a sample for the infrared imaging acquisition and processing techniques.

1.3 Research Significance

In previous studies, various non-destructive WDN leak detection techniques were employed. Some of these methods showed uncertainties, inaccuracies, and limitation to work only in a laboratory setting.

Although the current methods had been used for decades, The water industry still lacks a comprehensive automated leak detection methodology that is practically applicable in real networks. This system is capable of near real-time leak detection, while saving significant resources for the water utility companies. In addition, the method is cost effective as it utilizes existing monitoring sensors in WDNs. Furthermore, having the system to be drone-based equipped with a navigation system would allow for automatic image geo-referencing and processing to identify the leak locations with the help of the GIS customized interface. The development of such a system is novel in the leak detection field of study, which has not been previously employed in research.

Chapter 2. Background and Literature Review

A variety of leak detection techniques have been proposed in the literature including acoustic, pressure or flow sensors, ground penetrating radars (GPR), infrared thermography, remote sensing, and electromagnetic waves methods. The following sections provide a summary of each method.

2.1 Acoustic Methods

Acoustic leak detection methods, which include leak-noise correlators and noise detection devices to recognize water as it escapes the system, had been adopted for years. Acoustic equipment were initially developed for use on metallic pipes, therefore, it can provide less accurate results when used on a plastic pipe [3]. Figure 1 illustrates the data collection process of the acoustic equipment. Yang et al. (2008) integrated the conventional acoustic technique with a neural network-based model in order to account for false leak signals. Results obtained were promising and showed a 92.5% leak detection success rate [11]. Ahadi et al (2010) attempted another approach by studying the Short Time Fourier Transforms (STFT) of AE (Acoustic Emission) signals over a long-time span.

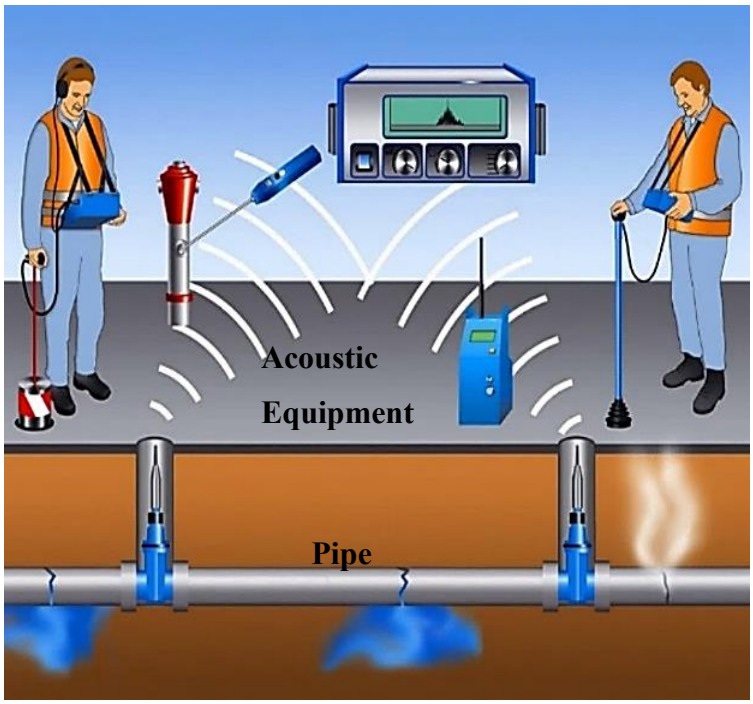

Figure 1: Acoustic equipment data collection process[63]

This information was then utilized to detect the time frame in which leakage was proved dominant which has helped in degrading the effect of false signals [12]. Gao et al. (2004) studied the effectiveness of pressure, velocity and acceleration sensors to detect leaks in plastic pipes. When evaluated using real water pipes, results showed that the pressure signals can be used for effective leak detection. However, such signals can be accompanied by various false leak signals as a result of measurement inaccuracies [13].

2.2 Pressure Sensors

Pressure sensors (Figure 2) is a widely used conventional leak detection method in which pressure sensors are built in pipes. It works by detecting the pressure drops throughout the WDN as a warning sign of leaks. Perez et al. (2009) placed various pressure sensors throughout a distribution network and formed a sensitivity matrix using the pressure sensor signals to detect the leaks. The results of the study showed various uncertainties that needed further investigation [8]. Mashford et al. (2009) used support vector machine (SVM) with pressure data, which has improved the detection accuracy, but remained inadequate for real-size WDN application [14]. Wu et al. (2010) were successful in detecting leakage nodes in a water distribution network by an optimization model based on a genetic algorithm that can enhance leak location using actual leak positions [15]. Casillas et al. (2013) examined the effect of extended-horizon analysis of pressure signals, and the results showed an improved leak location accuracy [16]. Christodoulou at al. (2013) presented a new method called greedy-search heuristic in order to optimize the localization of sensors as well as test the accuracy of leak detection. This method is based on the maximality, subadditivity and equivocation properties of entropy. Results showed that this method has uncertainties and require adjustments [17]. Sala et al. (2014) proposed an integrated leak detection method based on flow control system, which is complimented by an electronic system that aids in remote transmission of data based on mobile communication (GSM) protocols. The results proved the success of the method in leak detection [18]. Chatzigeorgiou (2014) developed an in-pipe leak detection system to locate leaks based on radial pressure gradient values. It was proved successful with a suggested further sensitivity enhancement [6]. A Head Loss Ratio (HLR) method was proposed by Ishido et al. (2014). This method uses a ratio of two differences of pressure measurements to detect the leaks and it was proven successful only to certain types of networks (e.g. Networks

with only one water source) [19]**.** Additionally, Sarrate et al. (2014) provided an optimization approach to identify the required set of pressure sensors which in turn would maximize the leak detection accuracy in WDN. Results showed that the method was efficient but could be further improved in the future [20]. Casillas et al. (2015) developed an optimization approach to minimize the number of overlapping signature domains computed from the original leak signature space (LSS) representation [21]. Similarly, Cuguer´o-Escofet et al. (2017) presented an algorithm to optimize the pressure sensor localization in the distribution network in order to maximize their effectiveness [22]. Soldevilaa et al. (2018) used a hybrid feature selection algorithm to identify the proper pressure sensor locations within the pipes based on previous pressure records. This method was applied to a small sized lab set up to observe its computational performance. Subsequently, it was tested on a medium scale set up to ensure its feasibility on large pipe sizes [23]. Saldarriagaa et al. (2015) utilized another optimization approach based on (Non-dominated Sorting Genetic Algorithm II (NSGA-II). This method helped in the localization of a set of pressure reduction valves (PRV) across pipelines to reduce leaks. A computational tool was developed in this study for method validation [24]. Another state-of-the-art wireless pressure detection sensor was developed by Sadeghioon et al. (2014) to spot leaks based on the measurement of relative indirect pressure changes in plastic pipes. This method can perform continuous monitoring without operator intervention [25]. The method was proved successful in detecting the locations of pressure changes in the WDN.

2.3 Flow Sensors

Fewer research was conducted on the utilization of flow sensor data to determine the leak locations within a network (Figure 2). It works by identifying flow drops in the WDN as they are indicative of leaks. Mulholland et al. (2014) employed a linear programing algorithm based on the network hydraulics to identify the leak spots using sparse flow data [26]. Farah and Shahrour (2017) proposed a real-time leak detection technique using traditional flow balance integrated with the minimum night flow (MNF) to provide flow thresholds for accurate leak identification. This method allowed for the reduction of future leaks by 36% owing to its capability of detecting leaks rapidly [27]. A similar study by Washali et al. (2018) computed leakage rate, components and reduction potential based on MNF and reduced leak frequencies [28].

Cabas et al. (2018) proposed a detection method that utilized non-linear partial differential equations and flow data for flow modelling and irregularities detection within the network for leak localization. The method was tested on a pilot scale model and provided reasonable leak location estimations [29]. Furthermore, a study carried out by Pal and Kant (2019) performed extensive simulations with the help of optimization models that use available flow data to locate possible leak spots within the system [30]. This review showed that majority of the studies that utilized flow data have presented lower accuracy results as compared to studies that utilized pressure data.

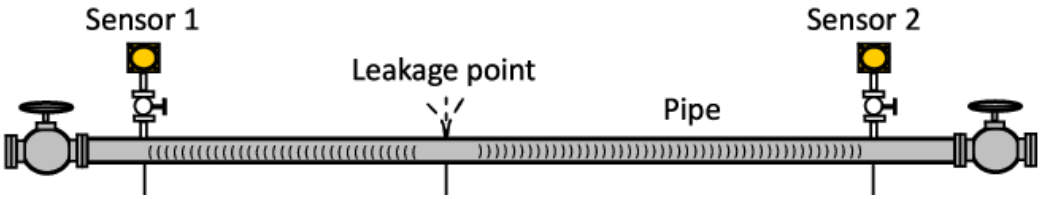

Figure 2: Sensor locations in pipes

2.4 Infrared Thermography

A remote alternative that requires increased attention in literature is infrared thermography. It is the use of an infrared camera to detect temperature variations across a surface using the emitted infrared radiation. Those images are then converted to a multicolored image that can indicate the thermal patterns across the surface. Leak locations are identified by the areas showing lower temperatures on the image (Figure 3). Fan (2005) examined the use of infrared imagery for the identification of leaks in pipes with and without pipeline heat isolation layer (PHIL). The effectiveness of the process had been verified [31]. Bach and Kodikara (2017) utilized the same technique and results indicated a 59% success rate of the available leaks, additionally, 22 % of the leaks showed notable, yet inconclusive, thermal signatures [32]. Fahmy et al. (2010) conducted field experiments using an infrared camera and developed a model to spot and locate the leaks in water mains. It provided successful results in the fall and spring seasons, but the model failed during summer due to high temperatures and also in winter due to snow dispersion [33]. Additionally, Shakmak et al. (2015) explored the

possibility of using high and low resolution infrared systems and found out results were positive irrespective of the resolution [34].

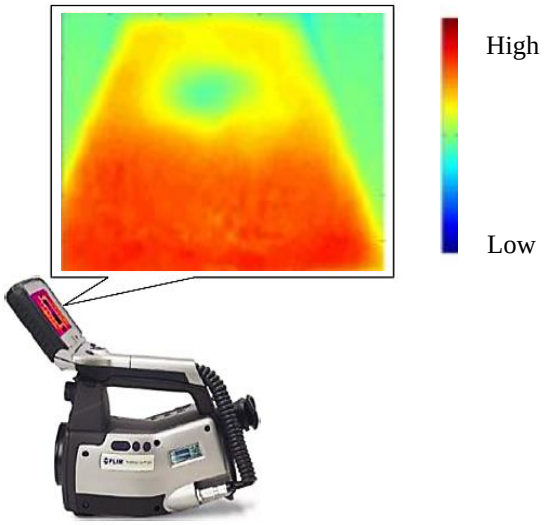

Figure 3: IR camera shows thermal contrast at pavement surface due to water leak

2.5 Ground Penetrating Radar (GPR)

Another approach to pipeline crack identification is ground penetrating radar (GPR), where an antenna provides electromagnetic waves through an object and is subsequently reflected back (see Figure 4). The waves received by the GPR are recorded to generate a profile representing the inspected object. Water leaks spotted as the pipe cracks would show irregularities in the created profile [9]. Atef et al. (2016) integrated the infrared photography with GPR techniques. GPR was used to locate the buried pipes, subsequently, the IR images were taken to identify the probable leak locations. Results were promising with an error percentage of 2.9–5.6%. In addition, a case study was carried out to determine the feasibility of GPR in leak detection, utilizing a software based on finite-difference time domain (FDTD) method [9]. The method successfully identified many leaks according to Nakhkash and Zadeh (2004) [35]. A pilot scale GPR was used by Hyun et al. (2008) to study lab simulated pipe leakage [36]. Bimpas et al. (2011) combined GPR with a decision support system (DSS) to manage the rehabilitation of the buried pipes. The study suggested further enhancement of the proposed system [37]. Cabrera et al. (2013) used GPR imaging to identify the pipe leakage features using a combination of statistical methods and multi-agent

system. In addition, the obtained features were utilized to test for leaks in a real water distribution network. The proposed system results agreed with the expected values [38].

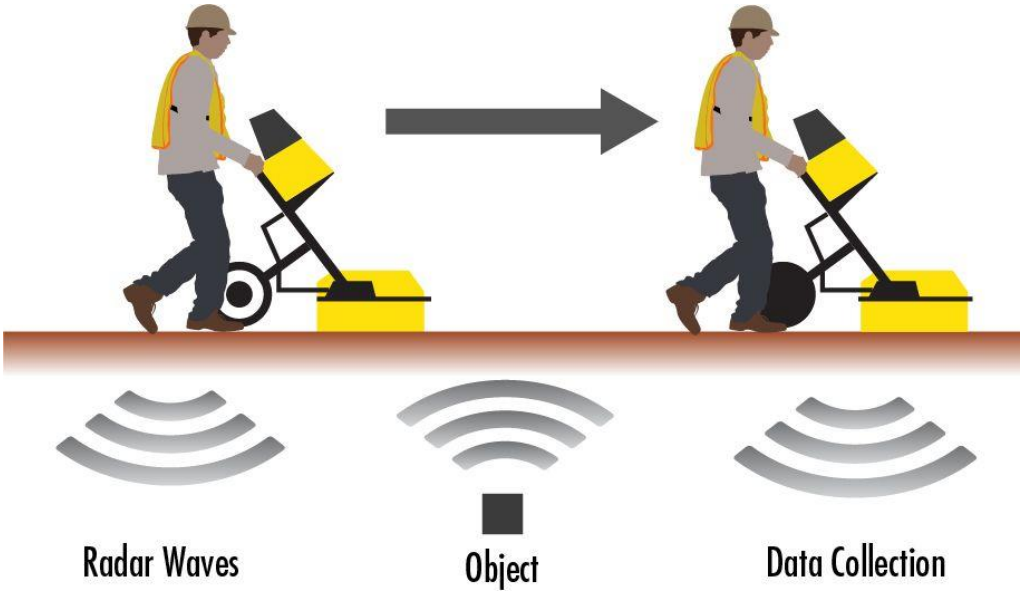

Figure 4: GPR data collection process[39]

2.6 Remote Sensing

Remote sensing (Figure 5) is typically the use of an aircraft or satellite to detect the physical characteristics of an area by measuring its emitted and reflected radiation from a distance. A study by Taylor et al. (2014) examined two remote sensing imagery, a

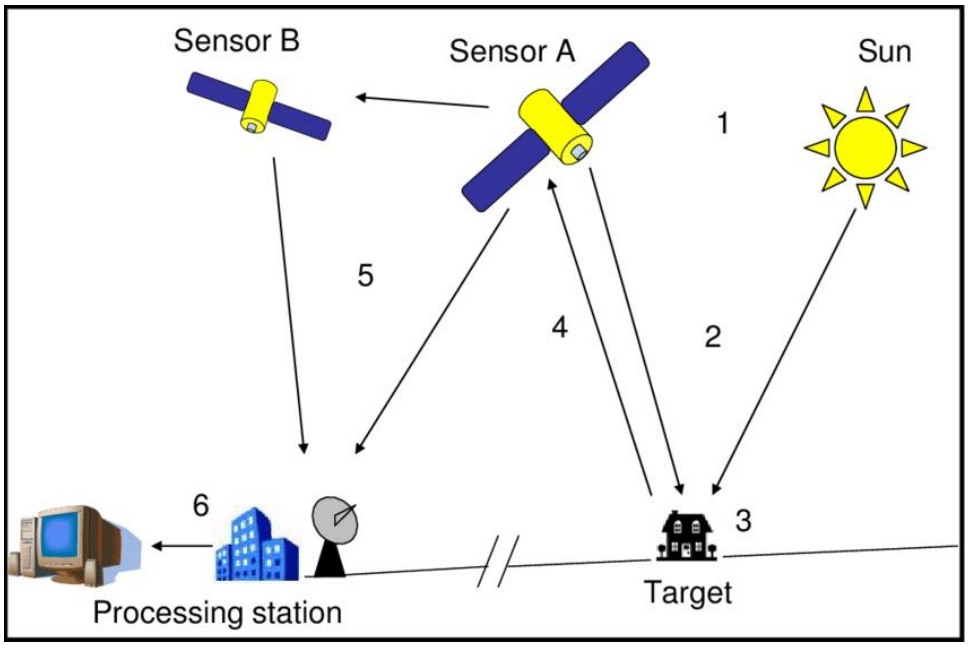

Figure 5: Remote sensing data collection process[40]

single high resolution QuickBird image or multitemporal SPOT images, on both an experimental scale and an actual 25 km long pipes, respectively. Normalized Difference Vegetation Index (NDVI) values were extracted in both cases and used for leak detection. The results proved the success of the method in the early detection of the leaks, specifically in unapproachable vicinities [41].

2.7 Electromagnetic Waves

This method works by utilizing electromagnetic sensors to detect the signals reflected by the pipes in real time. These sensors detect the irregularities in the received signals in case of a leak. Muggleton et al. (2003) derived pipe equations based on two axisymmetric wave types: fluid dominated wave and an axial shell in a plastic pipe with full flow enclosed by an infinite elastic medium [42]. Another study (Covas et al. (2005)) focused on the standing wave difference method (SWDM). The method was applied to several pipe arrangements and sizes, the pressure peak was identified and correlated to the frequency measure by the SWDM method. The technique was found promising although it can difficult to use in to a real scale network [43]. Brunone (2003) used wavelet transform which uses the pressure data of the distribution network. This method can spot singularities in the pressure time history as a result of the presence of a leak, which normally causes discontinuity in time. This can be used in the identification of the arrival time of the leak reflected pressure wave [44].

Table 1 summarizes the various leak detection methods, which have been discussed in this section. The table presents the advantages and disadvantages of each method for leak detection in WDNs.

Table 1 Summary of the leak detection methods

Technique	Significance	Limitation	References
Acoustic Equipment	• Real-time detection. • High accuracy.	• Low accuracy in noisy situations. • Loss of time information. • Absence of mathematical reliability. • Slow process.	[3], [13], [11], [12]
Pressure Sensors	• Pressure drops are directly related to leaks. • Zero cost since the sensors are already installed in the network.	• Other factors affect pressure readings, yielding false leak alarms. • Determining the optimal sensor location is a challenging process	[8], [14], [15], [16], [17], [18], [6], [19], [20], [21], [23], [24], [25]
Flow Sensors	• Zero cost as sensors are built in the pipes.	• Other factors affect flow readings, yielding false leak alarms. • Limited studies conducted.	[26], [27], [28], [29], [30]
GPR	• Works for all pipe sizes and materials.	• Time consuming. • Responds differently to changes in soil types	[9], [35], [36], [37], [38]
IR Thermography	• Covers large areas of land. • Cost effective.	• Requires experienced labor • Affected by soil moisture and overall weather conditions.	[31], [32], [33], [34]
Electromagnetic Waves	• Effective in detecting leaks in lab scale experiments.	• Difficult to implement on a real scale network. • Inaccurate.	[42], [43], [44]

Chapter 3. Methodology

The methodology developed in this research combines sensor measurements of drops in pressure, flow and chlorine (as a water quality indicator) to identify possible leak locations utilizing GIS tools. Pressure, flow, and chlorine levels are typically monitored in WDNs with sensors installed across the network. The sensor readings of these parameters were used in this research to identify the WDN locations most vulnerable to leaks. Subsequently, infrared (IR) images of the possible leak locations were acquired with an IR camera. These images were then processed to identify leak locations. This leak detection method has been automated by developing a customized GIS interface. Figure 6 shows the workflow of the proposed system. The following sections provide details of the method developed in this study.

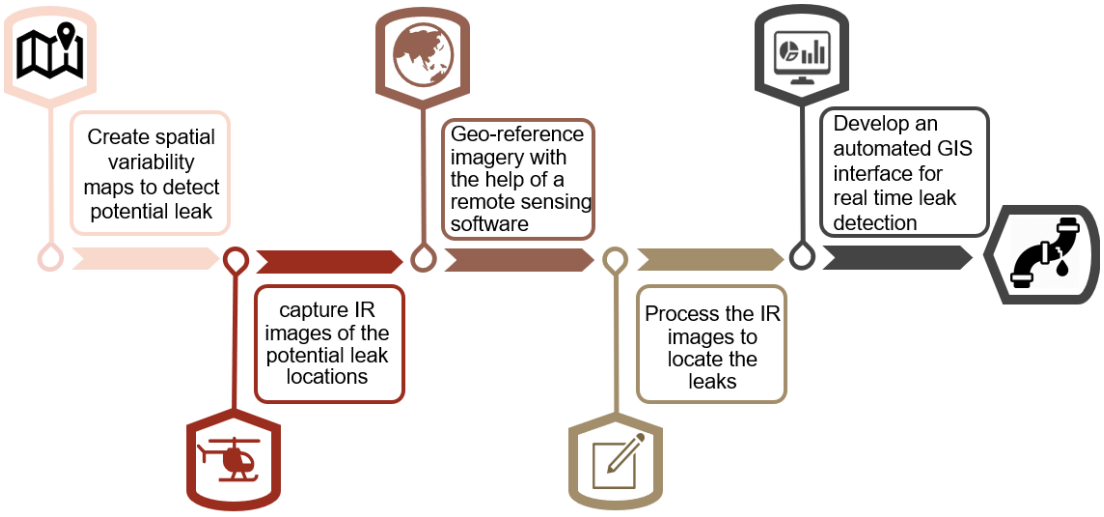

Figure 6: The proposed system architecture

3.1 Study Area

The method developed in this study was tested on the WDN of the city of Sharjah. The network information and sensor measurements were provided by the Sharjah Electricity and Water Authority (SEWA). Figure 7 shows the SEWA WDN and the locations at which water quality parameters (e.g., chlorine, pH, temperature, etc.) in the network are measured. The pipe network consists of approximately 70,000 nodes, and the pipeline

extends to about 3,000 km throughout the entire city. Water in Sharjah is obtained from ground water and desalinated seawater and pumped into the WDN through three main treatment plants: Layyah, Hamriyah and Sajja. Chlorine is further injected into the network as a secondary disinfection treatment. The WDN is subdivided into 13 zones, each of which contains one or multiple pressure, flow, and water quality sensors. Sensor readings are recorded from the 13 monitoring zones on a daily basis to ensure the best quality of supply and to allow for anomaly detection. In this study, the proposed method was developed using data collected by SEWA for the span the year 2019-2020.

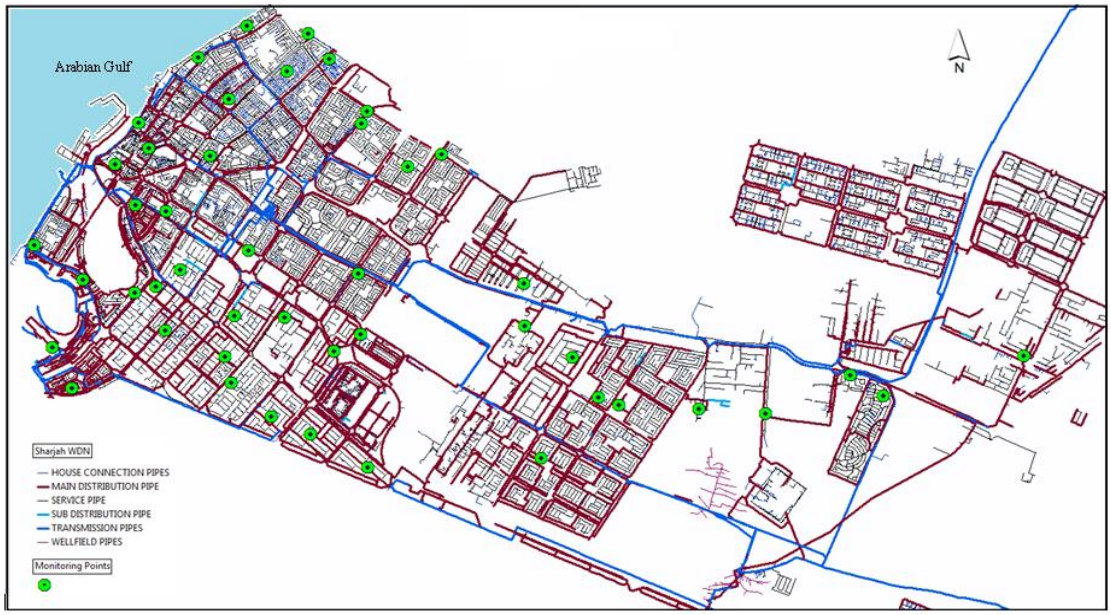

Figure 7: Water distribution network of Sharjah Electricity and Water Authority

3.2 Pressure Analysis

Pressure is identified in literature as the parameter being most indicative of leaks [45]. When a pipe wall cracks, the pressure within the network is disturbed causing pressure drops in the pipe as the water escapes from the pipes. SEWA's WDN is monitored by 13 pressure sensors placed in 13 zones, each of which records the pressure in 15-minute intervals. However, the data provided for the other parameters (i.e.: flow and chlorine levels) consists of a single value per day. Therefore, average daily pressure values were calculated in order to match the daily flow and water quality data provided by SEWA. Pressure drops in the WDN are influenced by many factors, these fluctuations remain

acceptable up to a certain limit of approximately 1.3 bar [46],[47]. This limit was used in this study as a threshold in the pressure analysis.

3.3 Flow Analysis

A leak is defined by the loss of water due to a defect in the pipeline, which in turn causes a reduction in the flow delivered to the end consumer [48]. Each zone in the network of the study area has single or multiple flow inlets and outlets. The quantity of water flowing through the system can be determined by the net flow, which is defined as the difference between the sum of water passing through the inlet and outlet points[11],[49].

$$Net\ flow\ =\ Inlet\ flow - Outlet\ flow \tag{1}$$

The daily inflow volume into a WDN is driven by the consumer demand. As the leak event occurs, the water flow through the pipe experiences a reduction, decreasing the outlet flow which is recorded by the sensor. Hence, in addition to the effluent, the net flow in this case would account for the water lost due to leaks (see Figure 8). Equation (1) can be rewritten as follows:

$$Net\ flow\ =\ Inlet\ flow - Outlet\ flow - Leak\ flow \tag{2}$$

Since the available data does not support the leak flow calculation as presented in Equation (2), the method instead uses areas of exceedingly large net flows as areas of suspected leaks.

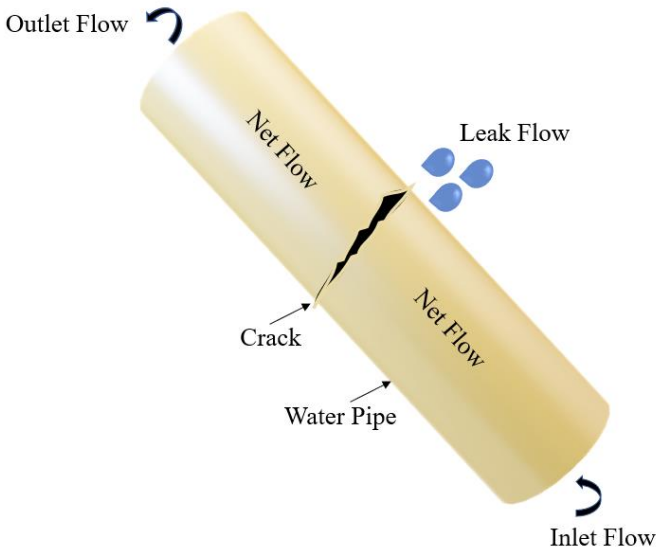

Figure 8: Pipe dynamics illustration in the case of leaks

The data provided by SEWA includes daily inlet and outlet flows for each of the 13 zones over the span of the year 2019-2020. In order to distinguish anomalous areas, monthly net flow averages were generated. The average net flow value of each month was applied as a threshold for the days to be examined within that specific month. Any values that were found higher than the average were used as indicators for possible leaks.

3.4 Chlorine Data

Chlorine is injected into the WDN and is used as a secondary disinfection [50]. This along with the maintained pressure is essential to keep the water free of contaminants. The SEWA network contains 46 water quality monitoring points distributed throughout the WDN (Figure 7). Various water quality parameters (temperature, pH, chlorine) are often monitored in order to determine the condition of the WDN, with residual chlorine being the most critical indicator [51]. The minimum acceptable residual chlorine levels should not fall below 0.2 mg/l under all conditions [52]. This constraint was used as a threshold to distinguish leaking areas in the WDN.

3.5 Spatial Variability Maps

Spatial variability occurs when a quantity at different locations throughout an area exhibits different values. Spatial variability maps are generated to display these variations over an area [53]. In this study, pressure and flow spatial variability maps based on inverse distance weighting (IDW) were generated using GIS to help identify the locations with relatively low parameter readings. Pressure and flow drops within the distribution system are often caused by leaks, which deteriorates the water quality in the WDN as a result. Therefore, in order to improve the accuracy of the results, chlorine residuals (as an indicative for water quality) values were examined at the suspected locations. Subsequently, overlay analysis in GIS was used to combine variability maps of flow and pressure drops. Overlay analysis is a process used to combine desired attributes from various layers into a single layer. The resulted layer was combined with the chlorine drop layer to identify the potential leak locations. A customized GIS interface was developed to automate the process and flag possible leak locations in near-real time as the as the sensor data is being processed by the system.

3.6 Customized GIS Interface

A GIS customized interface was developed for the leak detection system using the ESRI's ArcGIS 10.6 model builder in order to automate the leak detection process. The workflow of the automated procedure starts by generating average daily values of the flow and pressure data and are then evaluated based on their average monthly and minimum acceptable values, respectively. Variability raster layers are then created for these parameters using the Inverse Distance Weighted (IDW) interpolation technique. These raster layers present the spatial variations of each of the parameters, at the pixel level, throughout the network. Overlay Analysis is then used to identify areas with simultaneous drops in flow and pressure. Finally, the residual chlorine levels at the areas identified in the previous step is obtained and compared with the minimum acceptable values. The areas with drops in flow and pressure that yet show low levels of residual chlorine are identified as potential leak areas. In the case of a leak in the WDN, this customized interface would provide a visualization of the potential leak locations overlaid with the WDN and roads layers. Then, IR images were taken for these locations. The following flowchart shows the workflow of the proposed water leak detection system (Figure 9).

3.6.1 Model Builder

The model builder module in ArcGIS 2.6 Pro was utilized to develop a customized interface in order to automate the leak detection process. The model builder is a tool used to create and modify geoprocessing algorithms. It displays the selected functions in a diagram format, chaining separate tools together in a manner which enables the output of one function to be the input of the subsequent one [54]. The GIS interface algorithms, illustrated in Figure 10, include symbols consisting of three colors, each of which represents a distinctive function. The oval shaped blue icon represents the variables to be processed (inputs), the yellow boxes represent the selected Arctoolbox functions and processes, and the oval green icons represent the results returned from each function. As shown in Figure 10, arrows are used to join the separate components of the flowchart.

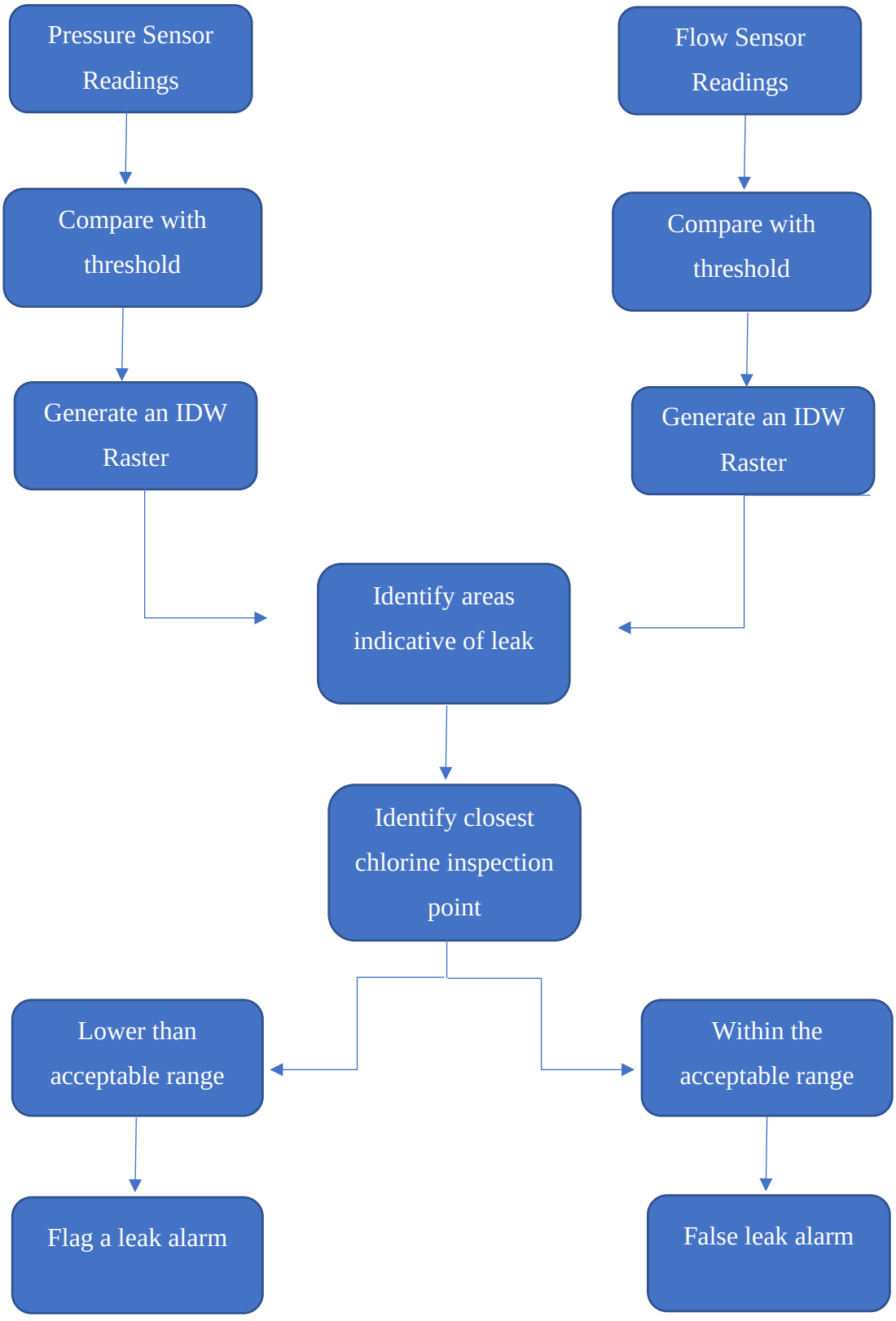

Figure 9 GIS Methodology flowchart

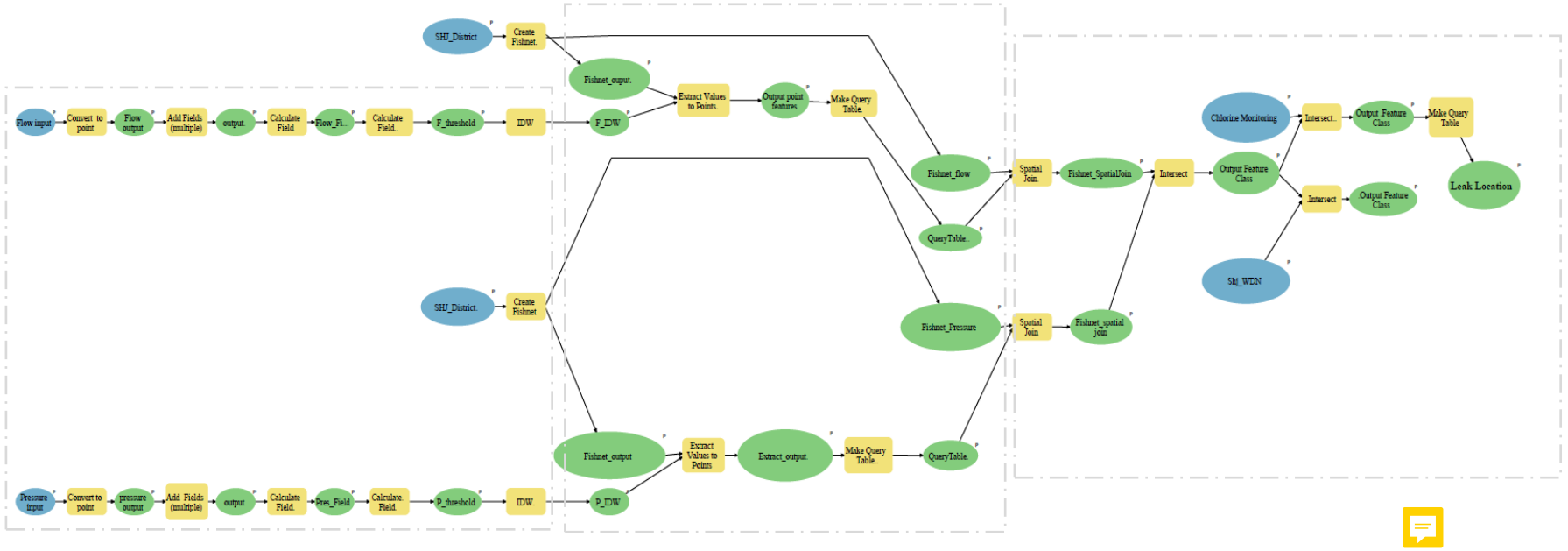
SHJ_District
Create Fishnet.
Fishnet_ouput.
Extract Values to Points.
Output point features
Make Query Table.
Flow input
Convert to point
Flow output
Add Fields (multiple)
output.
Calculate Field
Flow_Fi...
Calculate Field..
F_threshold
IDW
F_IDW
Fishnet_flow
QueryTable..
Spatial Join.
Fishnet_SpatialJoin
Intersect
Chlorine Monitoring
Intersect...
Output Feature Class
Make Query Table
Output Feature Class
Leak Location
Intersect
Output Feature Class
Shj_WDN
SHJ_District.
Create Fishnet
Fishnet_Pressure
Spatial Join
Fishnet_spatial join
Fishnet_output
Extract Values to Points
Extract_output.
Make Query Table..
QueryTable.
Pressure input
Convert to point
pressure output
Add Fields (multiple)
output.
Calculate Field.
Pres_Field
Calculate Field.
P_threshold
IDW.
P_IDW
Step 1
Step 2
Step 3

(a)

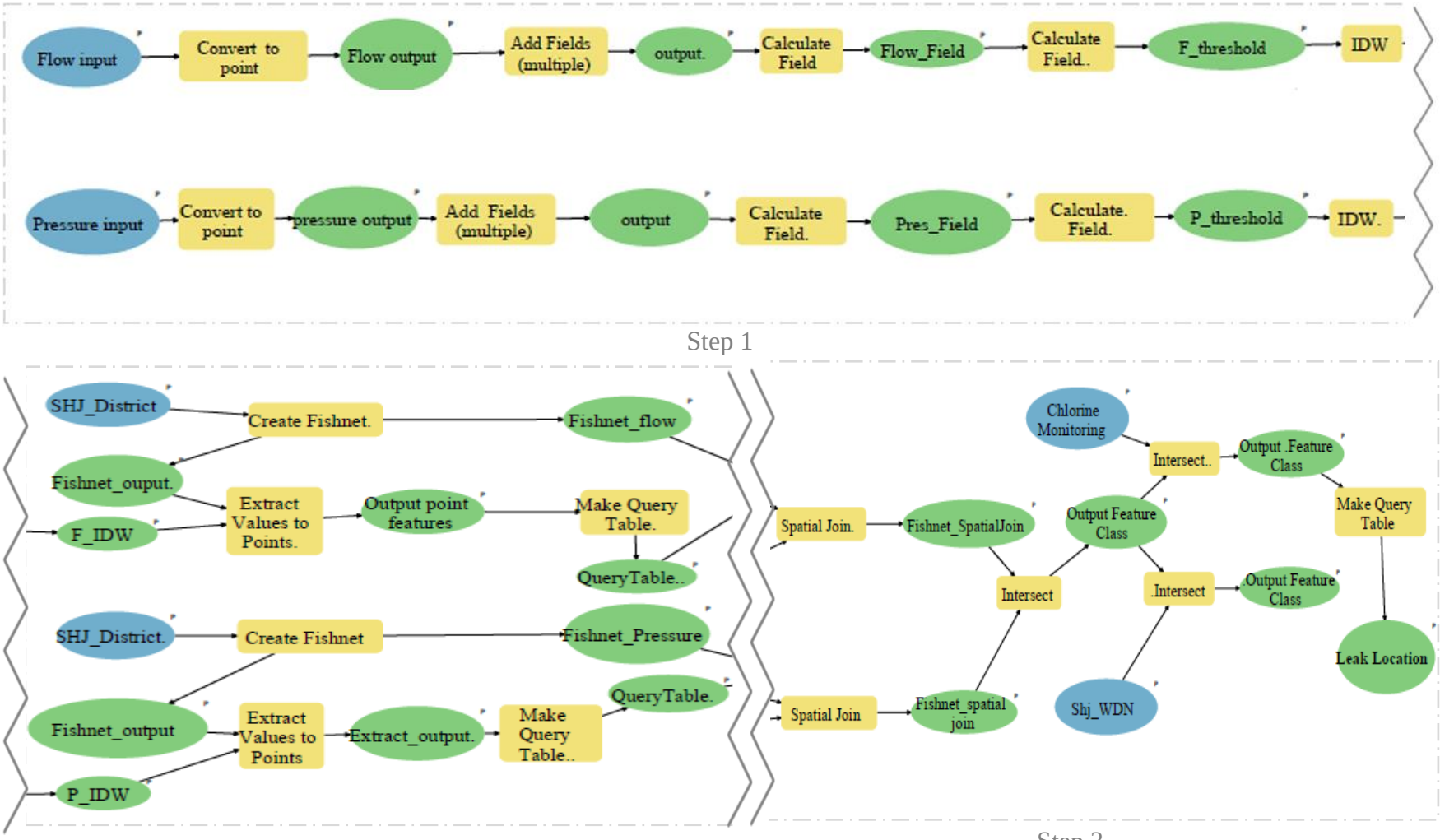

(b)

Figure 10: (a) GIS algorithms for automation of leak detection, (b) broken down into three steps

3.6.2 Model input variables

The inputs required for the model to run is, a layer displaying the boundaries of the study area, a layer of the WDN within the selected boundaries, and daily flow, pressure and chlorine data for the inspected month.

3.6.3 Model functions

The pressure and flow data were analyzed and inputted into the GIS interface. Each of the flow and pressure layers were compared with the thresholds discussed in the previous sections. Subsequently, raster layers were then created for each of the two parameters (flow and pressure) using the IDW interpolation technique, which is used to estimate the values of the two parameters at unsampled locations. Following this procedure, a fishnet mimic of the area was created in order to select certain portions of the network using GIS tools based on the thresholds of the analyzed parameters. Each of the mentioned steps were applied to the pressure and flow data individually. Similar tools were later employed to select the parts of the WDN pipes experiencing drops in the values of these parameters. Then, the potential leak locations were identified by intersecting areas with drops in both pressure and flow. Finally, GIS tools were used to locate the chlorine values in the areas that were identified in the previous step. Areas with drops in flow and pressure were mapped to the nearest chlorine station in the attribute table. Furthermore, these values were compared with the minimum acceptable value of chlorine using the attribute table to further narrow down the leak locations. The role of each of the main processes employed in this study are discussed below.

3.6.3.1 IDW interpolation

IDW was used in this research to determine the pressure, flow and water quality values at un-sampled locations based on the available point data. The IDW function uses the network borders to create a continuous surface raster of the area using a linearly weighted combination of inverse distance to the sampled locations (control points). The IDW method is based on two assumptions: 1) the value of the parameter at an unsampled location is impacted more by the values at the closest sampled points than the farther ones. 2) the extent of the impact (weight) of points on each other is proportional to the inverse of the distance between the points raised to a power. The process can be described by the following equation [55]:

$$Z = \frac{\sum_{i=1}^{n} W_i Z_i}{\sum_{i=1}^{n} W_i} = \frac{\sum_{i=1}^{n} Z_i / D_i^p}{\sum_{i=1}^{n} 1 / D_i^p} \quad (3)$$

where Z is the interpolated value, W_i is the weight that determines the relative significance of each of the adjacent sampling points (Z_i), Z_i is the value at the sampling points i = 1, .., i=n, n is the total number of sampling points available (12 values and above), D_i^p is the distance from the sampling point i to the interpolated point and p is a positive real number called the weighting exponent. When p = 1 the process is called inverse distance weighting (IDW), when p = 2 the method is called inverse square distance weighting (ISDW). In most weighting functions the default p value used is 2 [56].

3.6.3.2 Fishnet creation

This process creates a grid composed of rectangular cells [57]. Creating a fishnet requires the user to specify the spatial extent, cell size and the angle of rotation of the net. In this research, the spatial extent applied was the study area boundary and the grid cell size was assumed to be 500 km. The resulted fishnet was utilized to extract the IDW values to be stored in a vector format, required for the steps following this process.

3.6.3.3 Spatial join process

This method involves appending attributes from the join features to the target features based on their corresponding spatial locations. In this study, the join features were the parameter values narrowed down using the thresholds applied in previous steps and the target feature was applying the fishnet. This function assigned each of the narrowed down IDW values to the centroid of each cell of the fishnet.

3.6.3.4 Intersection

This process computes the geometric spatial intersection between the input features and returns portions that overlap in all layers to the output feature class. It Discovers geometric relationships (intersections) between features from all the feature classes or layers. Writes these intersections as features (point, line, or polygon) to the output. This method was employed several times in the automation model to intersect the suspected areas of leaks based on different parameters and subsequently overlay those areas with the network lines to identify the specific parts of the network to be inspected.

3.7 Infrared Thermography

Infrared (IR) thermography is the process of acquisition and analysis of thermal information emitted from an object, using thermal imaging devices. IR thermography detects radiation in the IR range of the electromagnetic spectrum, which corresponds to longer wavelengths compared to the visible segment of the spectrum. This in turn allows thermal imaging to detect information that might not be visible. An IR camera was used to detect temperature variations across the surface using the emitted infrared radiation. Leak locations were identified by the areas showing lower temperatures on the image. In this study, infrared thermography was used to detect these cold spots, which was used to identify leak locations. In the first part of the method, potential leak areas were selected using GIS considering drops in pressure, flow, and chlorine. The areas selected in the previous step were to be further investigated using IR images to identify exact leak coordinates.

It was initially proposed to acquire the IR images by a drone for the suspected leak area of the Sharjah WDN. However, due to the pandemic restrictions, the drone work was replaced with a pilot WDN, which was built outside the laboratory in order to complete the image acquisition and processing phase of the study. The WDN was built outside the laboratory in order to simulate the real-world environmental conditions. In addition, an IR camera was placed on a wooden frame at an appropriate height above the setup to capture the images (Figure 11). Subsequently, a faulty joint was introduced to the system to simulate the leaks. IR thermograms were captured, and various image processing approaches were attempted in order to achieve the most accurate image interpretation. The subsequent sections explain the pilot setup, camera frame, and the detailed analysis.

3.7.1 Lab setup

A lab setup was built to mimic a section of a WDN (Figure 11). The setup was made of a sand filled box, which had undergone 90% compaction. Additionally, 15 in Polypropylene (PPR) pipes were submerged at 16 in below the surface and placed 12 in apart. The pilot WDN was placed in an open site in order to be exposed to the actual environmental conditions of the UAE. Additionally, a faulty joint was introduced to the network so as to simulate a leak scenario to be captured by the infrared camera. The system included a secluded water tank, a pump, and a pressure gauge in order to

maintain and monitor the water flow throughout. An FLIR T420 infrared camera, with a wavelength of 7.5-13.0µm and a spatial resolution of 0.15×0.15cm^2, was used to perform the thermal imaging process. The IR camera was placed on a fixed wooden stand at a height of 1.5 m to capture the required images. Figure 11 and Figure 12 illustrate the pilot WDN setup and the camera frame. (Table 2) shows the detailed parameters of the pilot WDN and the way in which the infrared camera was fixed.

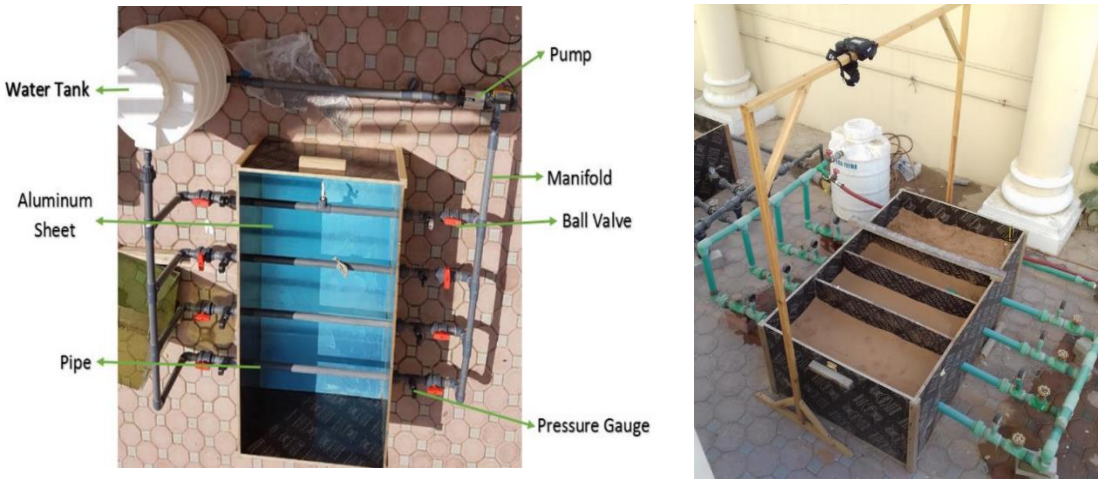

Figure 11: Experimental Setup: Top view

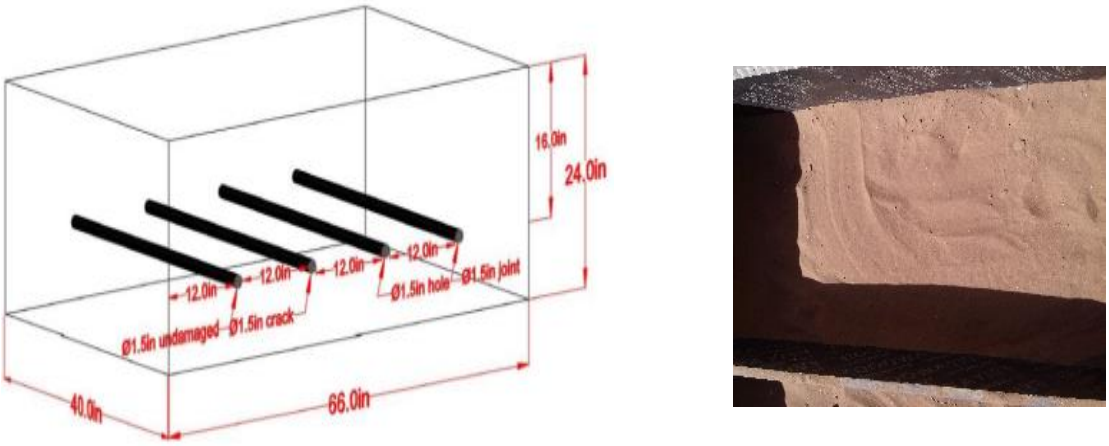

(a) (b

Figure 12: Experimental Setup: a) Dimensions b) initial image

Table 2: Lab setup details

Pipe Parameters	**Value**
Material	Polypropylene (PPR)
Diameter	1.5 in
Depth	16 in
Leak	Faulty joint
Water parameters	**Value**
Temperature	21°C
Pressure	0.5Pa
Water leakage	14 amp
Soil	**Value**
Type	Dune sand
Compaction	90%
Density	(1689.41 kg/m^3)
IR camera parameters	**Value**
Type	FLIR T420
Wavelength	7.5-13.0µm
Emissivity	0.98 (dry soil)
Height from the soil	1.5 m
IR image parameters	**Value**
Temporal resolution	1 image/ min
Spatial resolution	0.15×0.15cm^2

3.7.2 Data acquisition

Figure 13 displays the infrared images captured during the experiment, where the simulated leakage is characterized by the areas displaying lower temperatures, as depicted by the darker contrast areas. The lab setup was exposed to the sun during the

experiment; however, a shadowed portion was identified. Shadowed areas can be mistakenly detected as leaks in an infrared image, but this issue was resolved during the data analysis. For the purpose of the analysis and processing, the images were captured in grayscale format. When represented in grayscale, the R, G and B image layers are equal, which allowed each layer to be selected separately for the analysis. The grayscale format provided an accurate bijection between the temperature and luminance, which has allowed for an accurate leak identification. Additionally, the false color image palettes were used for visual inspection and to enhance the contrast of the thermograms (see Figure 19 : a, d & g). However, those palettes do not ensure a bijection between temperature and the RGB layers and the processing of a single false color layer is not ideal. Therefore, the grayscale images were used during this experiment instead [58].

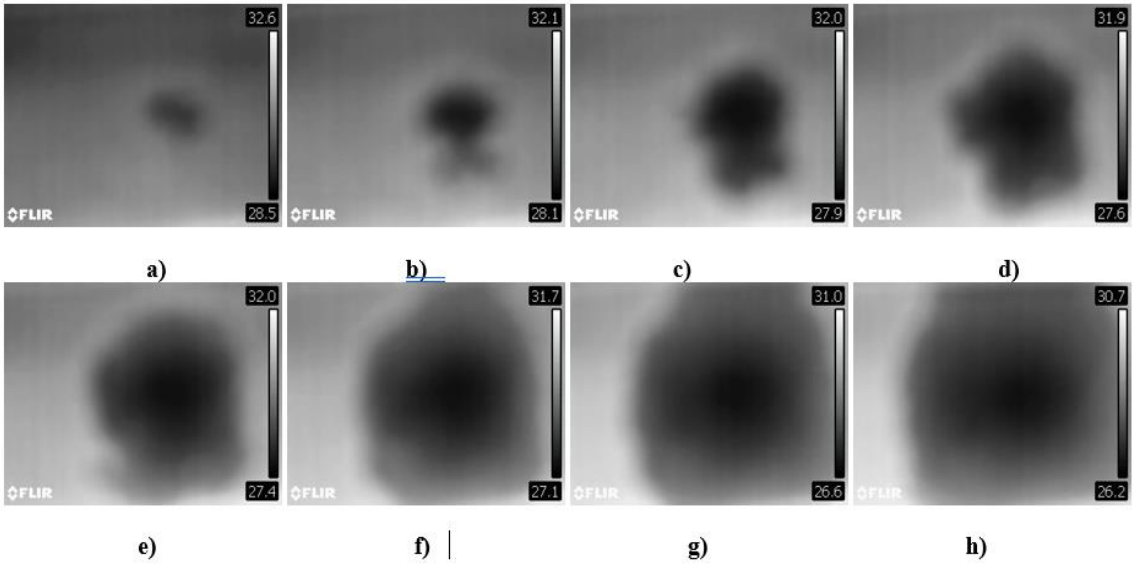

Figure 13: IR images detecting temperature in Celsius

The methodology of this section was refined throughout the experimentation process in order to obtain the optimal results. The image acquisition and processing part of the method proposed in this research can be summarized as follows (see Figure 14):

- *Acquisition of multitemporal IR images:*

The first step of the proposed leakage detection technique is the acquisition of the multitemporal IR data. Multitemporal IR imagery are images that are captured over

time at specific time intervals. When processed, such imagery would not only capture the leak and its location, but also the evolution of the leak over time.

- *Compute the norm image:*

  This step involves the computation of the mean of the 3x3 neighborhood of all pixels in the image.

- *Derivation of the threshold:*

To detect and locate the leakage zone, the threshold is calculated as function of the number of pixels of the leakage zone selected by the user.

- *Generation of the classified image:*

Let the class labels be denoted as, (0) and (1), which represent the classes of object (i.e., leakage) and background (i.e. non-leakage), respectively. Leakage and non-leakage pixels are identified by comparing each pixel of the norm image with the threshold. If the norm pixel value is higher than the threshold "TH", it will be assigned to the non-leakage class (0), else the pixel is assigned to the leakage class (1).

$$\text{Class}(i,j) = \begin{cases} 1(\text{Leakage}) & \text{if NORM}(i,j) < \text{TH} \\ 0\ (\text{Non} - \text{leakage}) & \text{elsewhere} \end{cases}$$

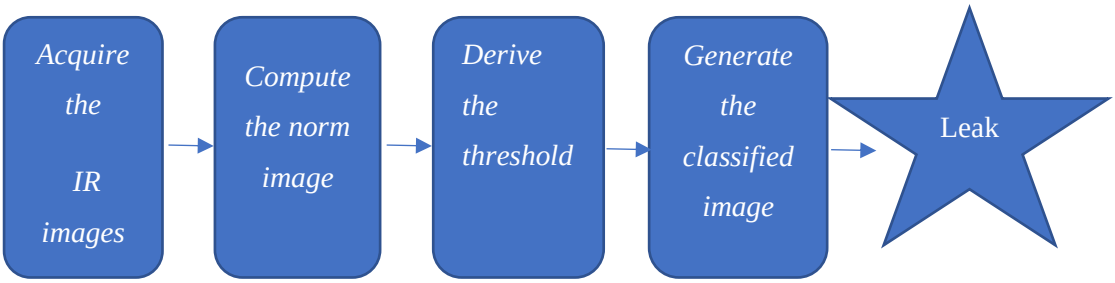

Figure 14 IR detection flowchart

Chapter 4. Data Analysis and Results

4.1 GIS interface

The automation process was carried out using ESRI ® ArcGIS Pro 2.6 utilizing the model builder tools. This process returns a series of visual outputs at individual functions. The first visual output was two IDW raster surfaces representing individual pressure and flow data points (sensor readings). Following this step, the locations selected to be indicative of leaks, based on numerical criteria, in each IDW were overlaid using overlay analysis and were subsequently intersected with the network layer as well. The next visual output was a capture of the chlorine monitoring points located in the vicinity selected in the previous steps. The chlorine values were further compared with the minimum acceptable limit (discussed in the methodology section) and the values that appeared to be within the limit were discarded from the map. The final visual output of the automation process then returns the network area showing drops in all three parameters that can indicate the presence of a leak. Figure 15 illustrates the series of outputs returned during the automation process.

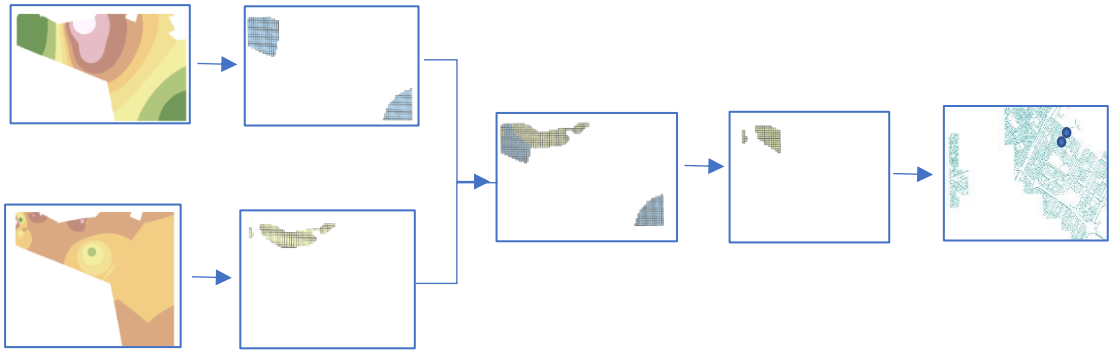

Figure 15 Series of model outputs

4.2 Temporal Analysis

The IDW method was employed to generate raster layers in ArcGIS presenting the spatial distribution of pressure, flow, and chlorine data throughout the study area. Three scenarios were carried out to evaluate the proposed method in leak detection. The first day of the months of October, January and July were selected to test the leak progression in water pipes throughout the seasons: Autumn, Winter and Summer, respectively.

4.2.1 Autumn analysis

For consistency, the first day of the month of October was chosen in this scenario to evaluate the proposed method. Figure 16 shows the resulted raster layers, obtained by interpolation using the IDW method, of pressure and flow data in the study area. The dark green color in Figure 16 indicates the lowest observed values and the white color indicates the highest. As shown in the figure, the pressure IDW raster layer returned by the model indicated low pressure values (0.6 to 1.2 bar) observed at few areas including: Butina, Al Ghuwair, Industrial area 4, Industrial area 6, Al Ghaphia, Maysaloon, Al Fayah and Al Nasserya. However, the remaining vicinities covering the Al Rahmaniya 1, Al Rahmaniya 3, Al Qadsia, Al Sabkha and Barashi indicated normal pressure behavior across the network (ranging from 2 to 3.75 bar). The IDW raster layer returned for the net flow data indicated a major increase covering the eastern sector of the network, which includes the following areas: Al Rahmaniya 1, Al Rahmaniya 3, Butina, Maysaloon, Al Nasserya, Barashi and Al Fayha while the remaining locations indicated normal flow patterns (110 to 7380 m^3/day). The individual pressure and flow drops were selected by the model (shown in brick red) and both of the selected areas in the pressure and flow layers were intersected. Since pressure and flow drops can be indicative of multiple defects other than leaks, the individual layers were intersected to determine the regions with higher possibility of a leak based on both parameters. Finally, a chlorine monitoring point showed a low chlorine value of 0.15 mg/l narrowed down the suspected area to a vicinity extending from Butina to Industrial area 4, including a pipe length of about 320 km.

4.2.2 Winter analysis

Day 1 of the month of January was selected to carry out this analysis. Figure 17 shows the spatial distribution, obtained from IDW, of pressure and flow throughout the study area. The dark green color indicated the lowest observed values and white indicated the highest values. The values of pressure varied between 0.67 to 4.07 bar respectively. As seen in the figure, areas including Al Rahmanya 1, Al Rahmanya 3 and Al Barashi pressure values were indicative of normal pressure patterns across that specific sector of the network. While, Al Sabka, Al Ghuwair, Industrial Area 4, Industrial Area 6, Butina, Al Qadsia, Al Nassreya, Al Ghaphia, Al Maysaloon and Al Fayah were displayed in dark green which reflected the highest pressure drops (between 0.6-1.0 bar) in the system. Hence, the dark green areas at the western and eastern ends were

selected (depicted in brick red) by the automation model of the proposed method to carry out further analysis. The IDW raster layer of the flow data utilized the same color patterns, with dark green color indicating the areas with highest net flow values (target) and white specifying areas with the lowest net flow. The net flow values within the study area fluctuated from 30 to 8000 m^3/day. Based on the daily averages calculated by the model for each area, the values above average were selected to be indicative of the leak. The suspected leak area (shown in brick red) was found to extend from Al Rahmaneya 1 to Al Ghuwair, including Al Sabka and Al Qadsiya. The remaining areas showed a relatively regular distribution of net flows within the network. The chosen areas based on pressure and flow data were overlaid to indicate the most vulnerable areas of the network, however, they were further intersected to determine the common areas where both flow and pressure drops were observed. Finally, two chlorine monitoring points, 0.2 mg/l and 0.14 mg/l respectively, were identified to be lower than the minimum acceptable value. As shown in the last step of the flowchart (Figure 17), the automation model selected the part of the network where a leak was identified based on the three parameters. This network section extended from Al Sabka through Al Ghafia to Al Ghuwair including a pipe length of around 480 km.

4.2.3 Summer analysis

The month of July was selected to carry out this run based on the data recorded on the first day of the month. Figure 18 illustrates the subsequent model outputs, which returns the final leak location specified at the last step. The raster layer obtained from the pressure data using IDW interpolation showed a varied pattern including pressure drops across most areas excluding Al Rahmaniya 1, Al Rahmaniya 3 and Barashi with pressure values varying from 0.65 to 2.3 bar. The net flow IDW represented relatively milder variations throughout the network based on the calculated averages per area, ranging from 950 to 8950 m^3/day. The areas selected by the automation model in step 2 from the individual IDWs of pressure and flow were somewhat similar indicating a high potential of leak in the observed locations. The layers were overlaid to determine the vulnerable sections of the network and further intersected to represent the vicinities that are at a higher risk. The total suspected leak area appeared to have drastically increased as compared to the previous runs. Finally, five chlorine monitoring points showing low chlorine readings were found to lie within the selected network section

(varying from 0.14 to 0.2 mg/l). The final step in Figure 18 represents the suspected leak location which extended from Al Sabkha to Industrial area 6 and beyond (1,500 km).

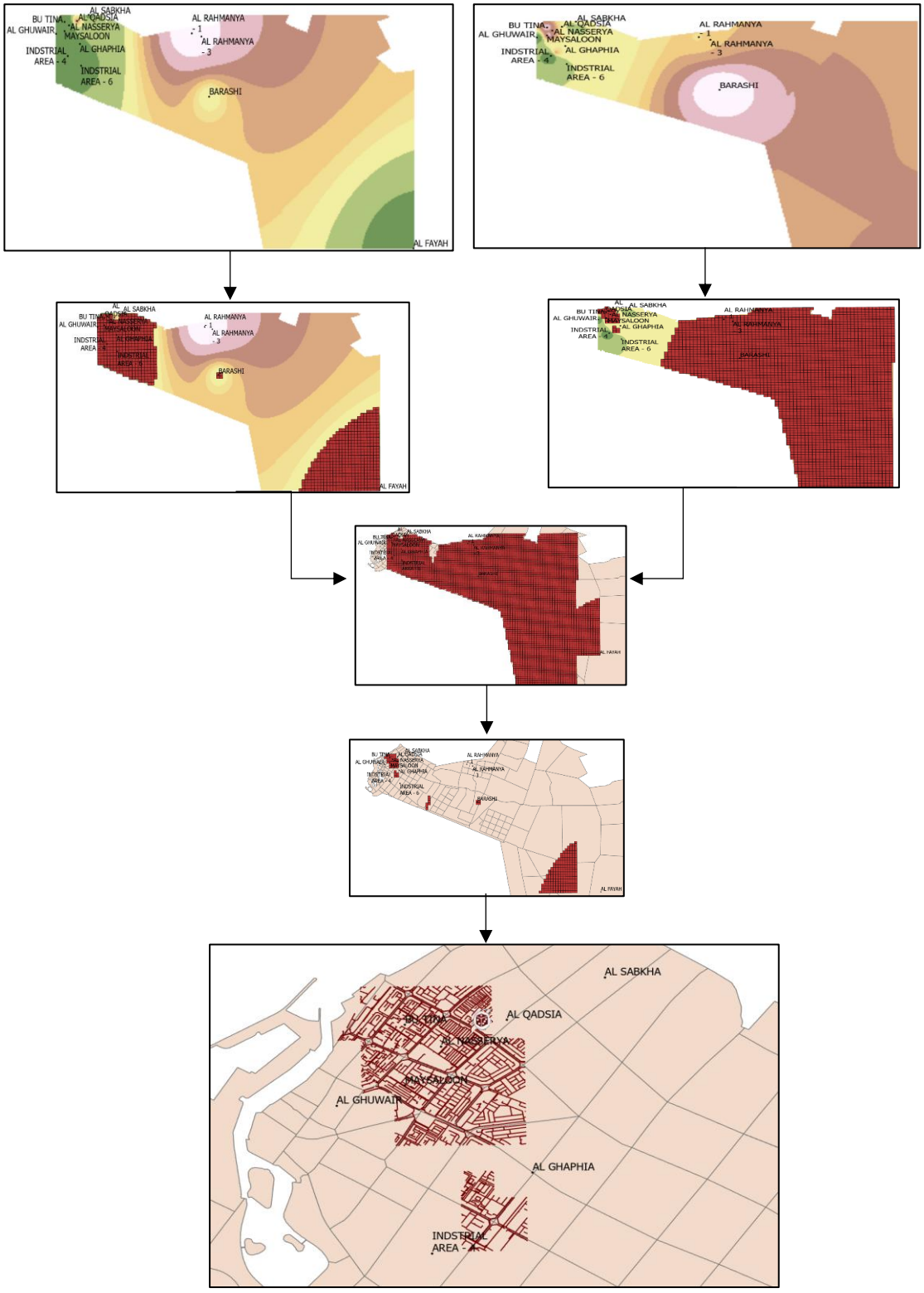

Figure 16 Analysis flowchart for the month of October

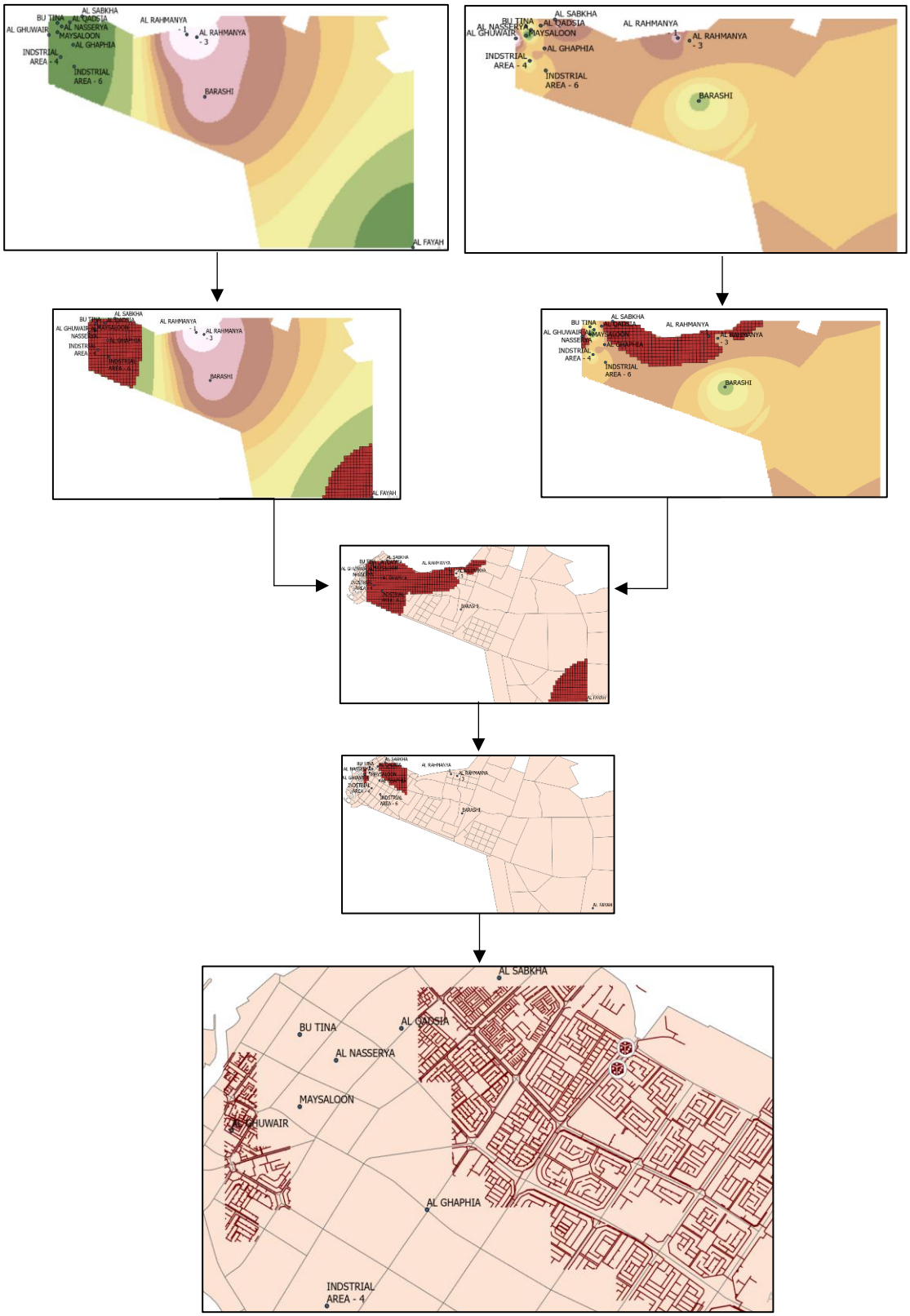

Figure 17 Analysis flowchart for the month of January

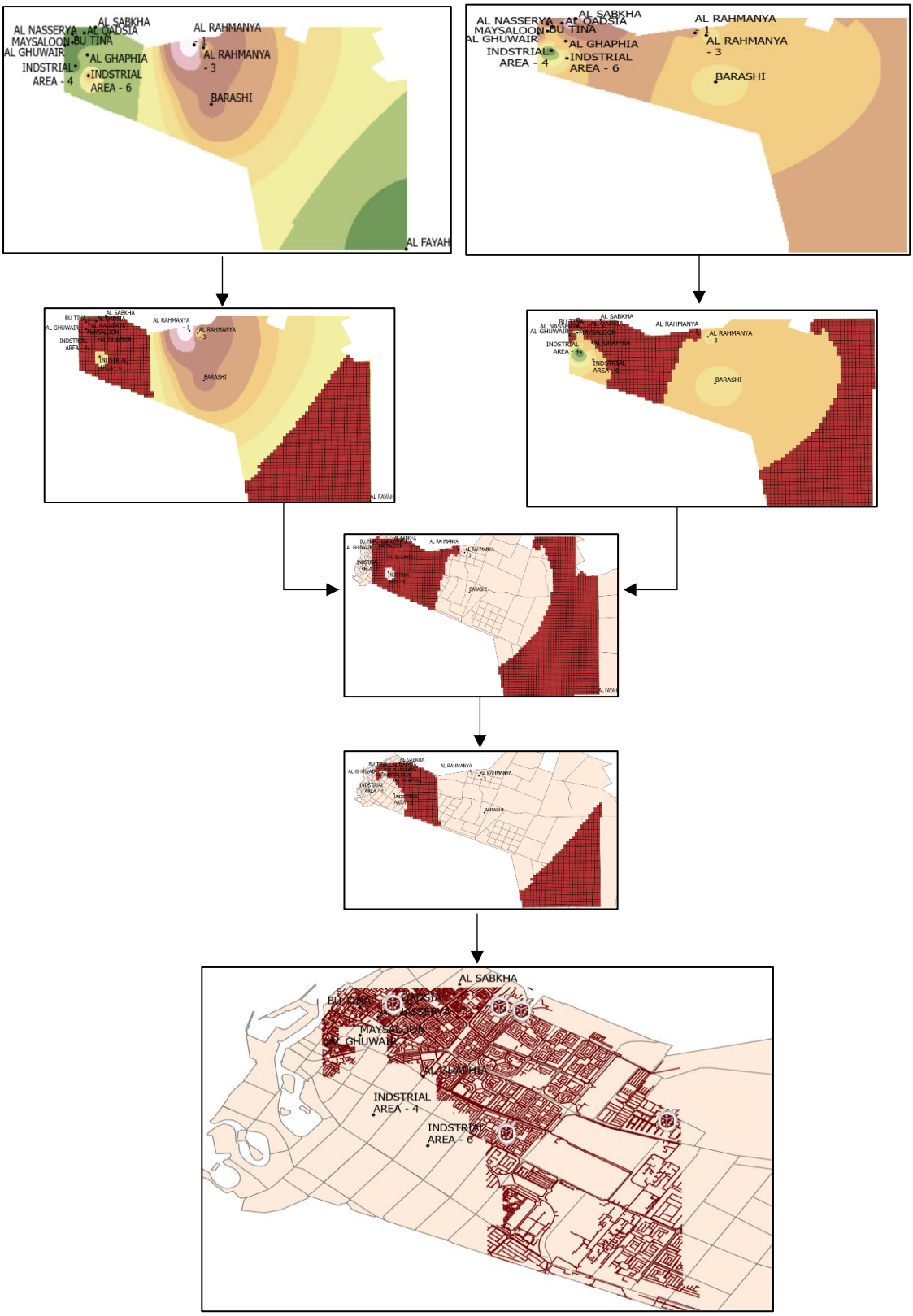

Figure 18 Analysis flowchart for the month of June

4.3 Infrared Thermography

Multitemporal IR imagery were captured for the pilot setup after simulating leakage. The image processing was caried out on MATLAB. When the IR images have low spatial contrast, are noisy or display small temporal changes, the visual inspection can fail to identify leakage areas (Figure 19: a,d and g). To resolve this issue, threshold-based algorithms were applied at this step. Thresholding is a type of image segmentation, where the pixels of an image are changed to make the image easier to analyze. In thresholding, images are converted from color or grayscale into a binary image, i.e., one that is simply black and white (Figure 19: c, f & i).

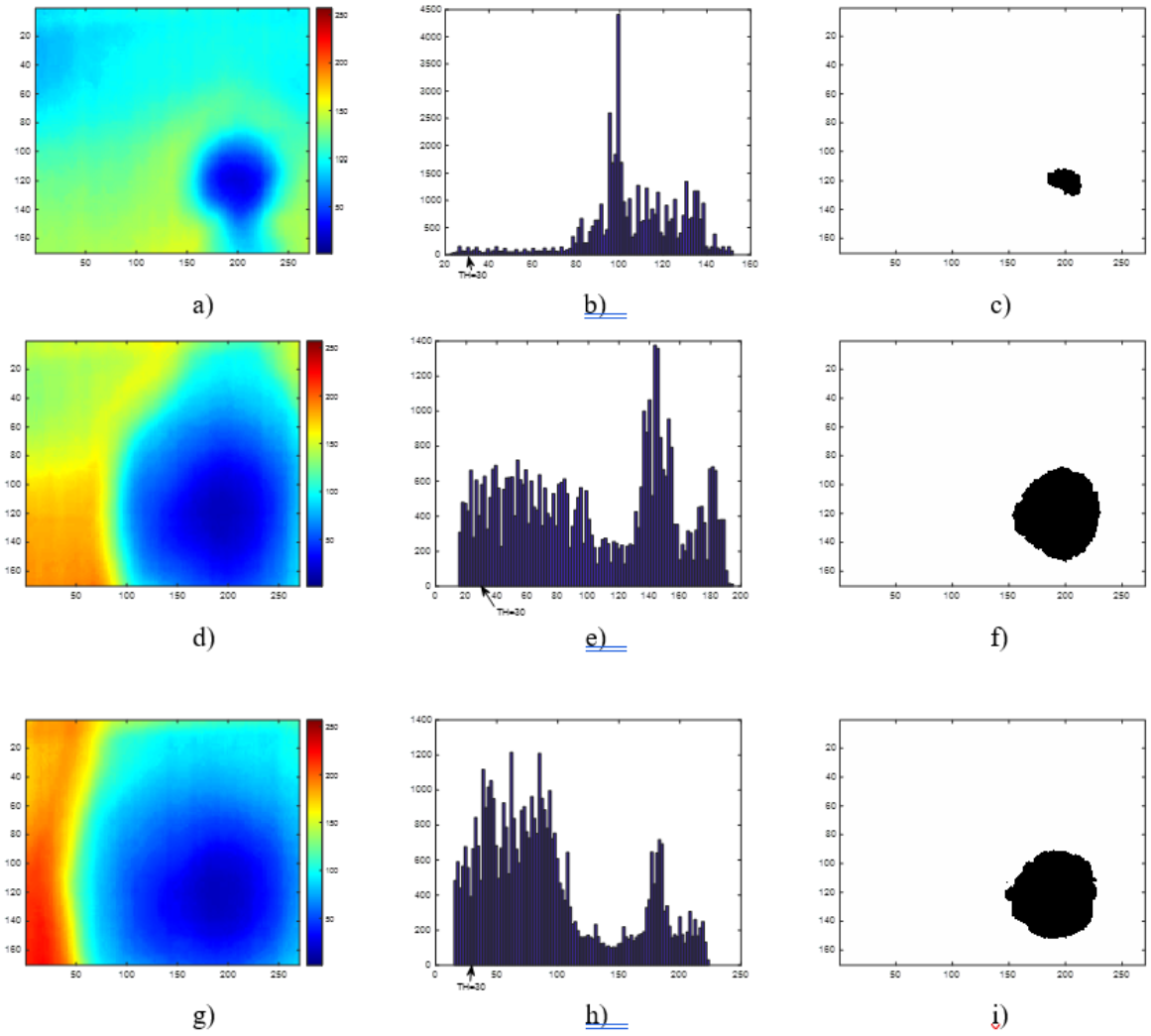

Figure 19: Fixed TH method, IR images, histograms, and leakage positions

Figure 19 displays the histograms of the acquired IR images, where 'TH=30' was initially used as a fixed threshold used to segment the IR images into leakage and non-leakage areas. It can be observed that leakage and non-leakage areas were

distinguished. Nevertheless, as indicated by the figure, the extent of leakage spots was varied considerably. To alleviate this limitation the threshold was adapted to the content of each of the IR images.

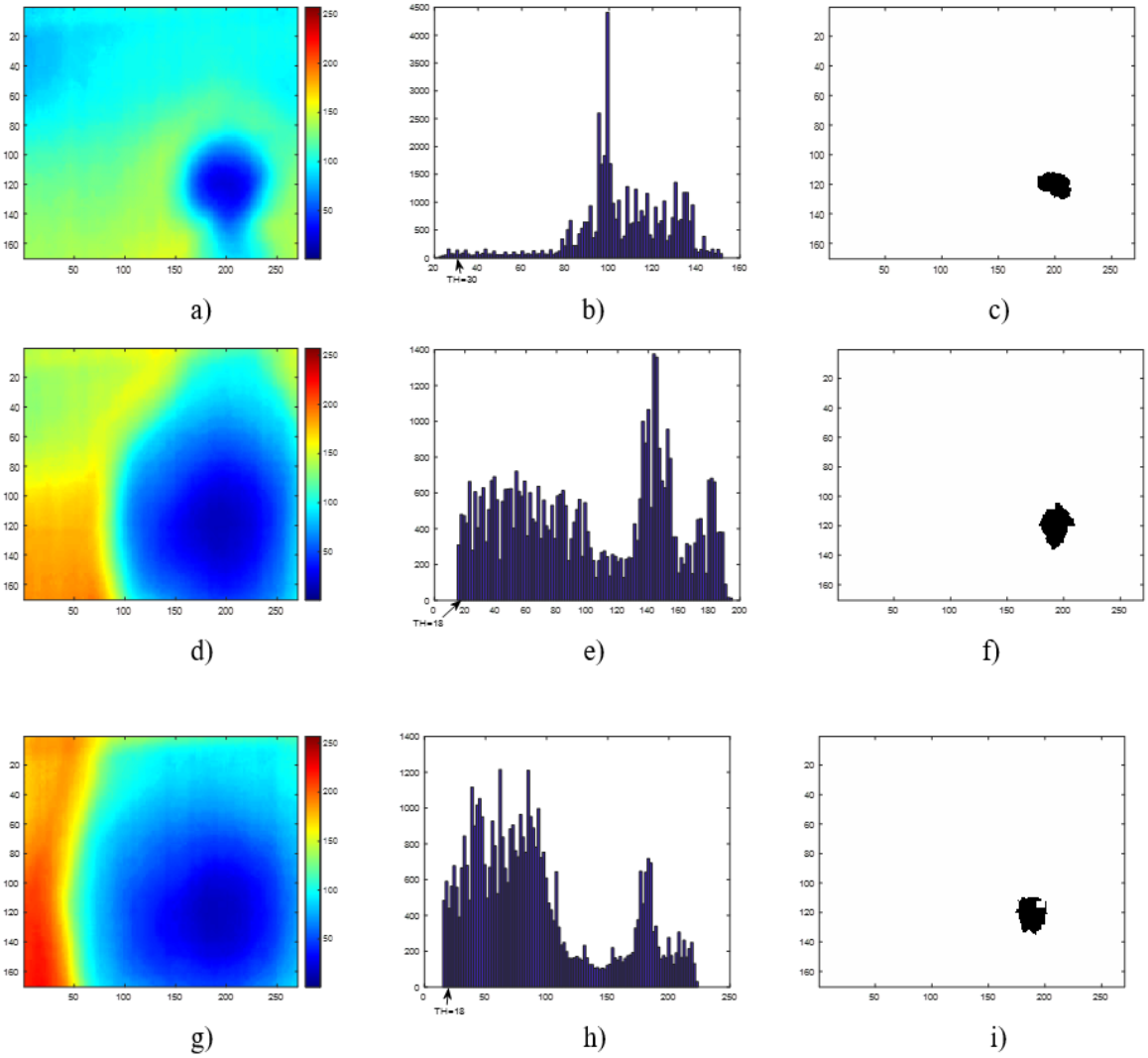

Figure 20: Varied TH method, IR images, Histograms, and leakage positions

(Figure 20) displays the histograms of the acquired IR images with varied TH values to accommodate the content of each image. It was observed that the extent of the leakage position of each image was varied compared to the initial attempt, and a considerable similarity in size between all the images was noted. However, the main limitation of this procedure is the requirement of the continuous intervention of the user to adjust the threshold for each image. Hence, an automated technique was required.

4.4 Proposed IR image processing approach:

4.4.1 Initial approach

In order to fix the size of the leakage positions, a definite number of the detected leakage pixels was selected. The selected number of pixels represents the pixels with the lowest temperature throughout the surface.

Figure 21 displays the classified images. The leakage zone was determined by two attempts, selecting 100 pixels (smaller extent) and 300 pixels (larger extent) with the lowest temperatures. It can be observed that leakage and non-leakage areas can be discerned, and the extent of the leakage area has been controlled. However, the main weakness of this method was that the detected zones are noisy and sparse. The values of noisy pixels can represent other environmental impacts which could be misclassified as leakage zones (e.g., shadows having low temperature).

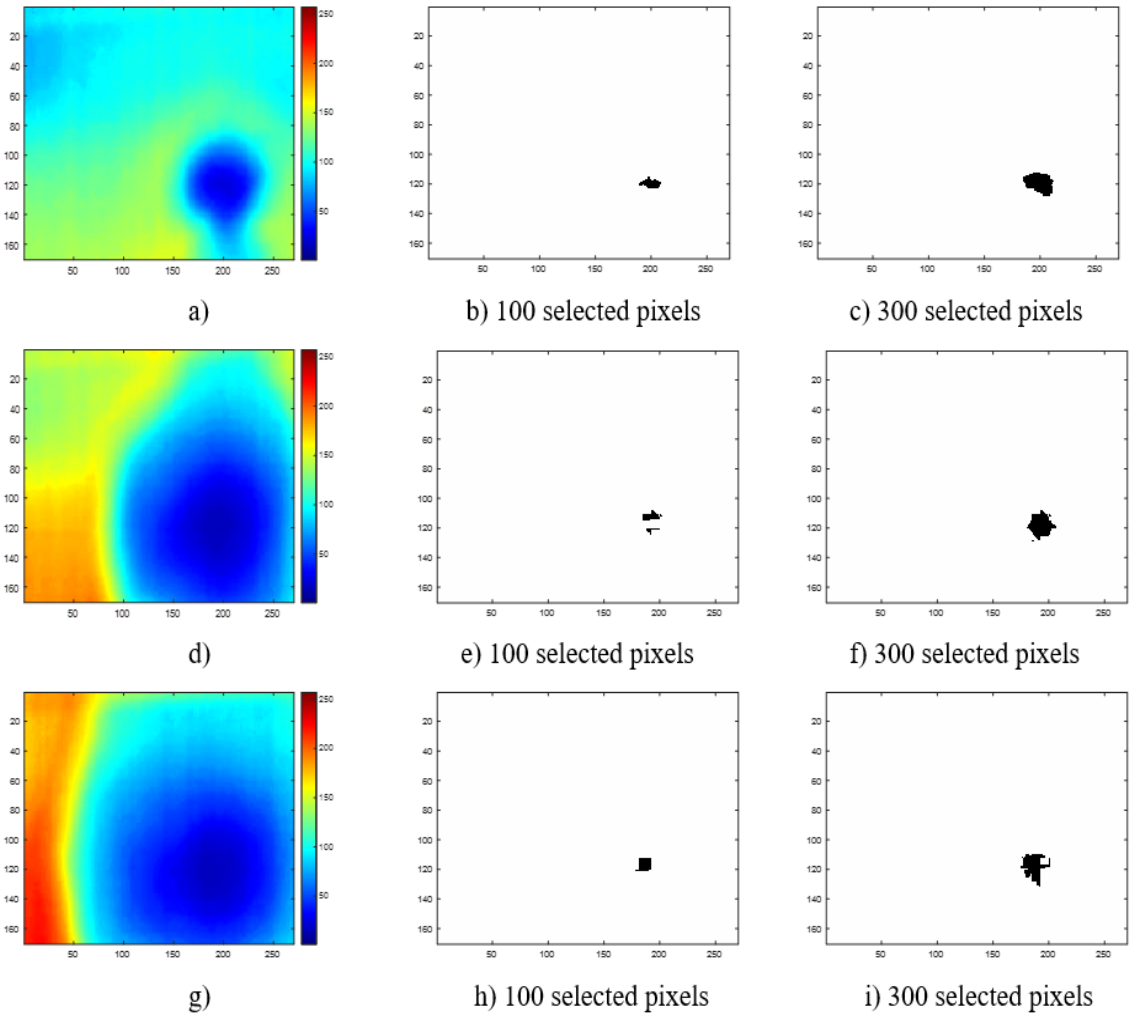

Figure 21: Proposed initial approach, IR images, Histograms, and leakage positions

4.4.2 Improved approach

Non-leakage noisy pixels having low temperature are characterized by high neighboring pixel values. Hence to exclude them, the norm (mean) of the values in 3 x 3 neighborhood was calculated for the image as a whole, using a 3 x 3 pixel window. Subsequently, the pixel values were substituted by the norm (mean) values of all neighbors. In this case, in a leakage zone, all pixels have low norm values. In non-leakage pixels, all pixels have high norm values even if the original pixel value was low.

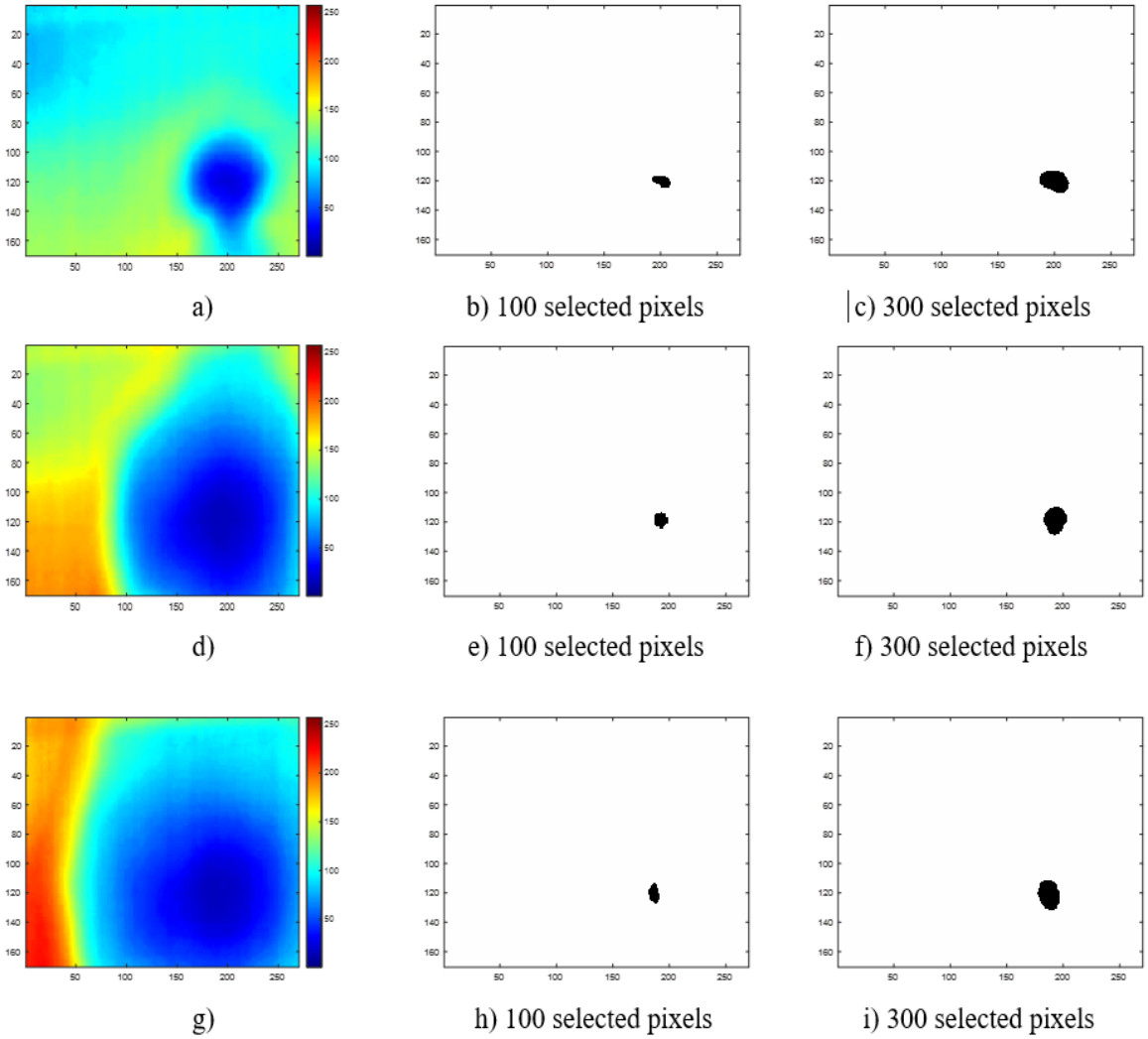

Figure 22: Proposed improved approach, IR images, histograms, and leakage positions

(Figure 22) displays the classified images. The leakage zone is determined by selecting the 100 and 300 pixels having lowest norm values. It can be observed that leakage and non-leakage areas can be distinguished. The extent of leakage localization has been controlled by excluding noise.

Chapter 5. Discussion

The proposed leak detection method in the WDN was successfully tested using a section of Sharjah WDN. The main objective of the test was to evaluate the efficiency of the method in identifying suspected leak areas. Results obtained from the analyzed data showed a gradual increase in the suspected leakage areas from the month of October to the month of July. This can be attributed to the extreme temperature fluctuations over the selected seasons in Sharjah, UAE. This indicates the presence of more pipe breakage/leakage in summer and winter compared to spring and autumn [59]. Additionally, the time factor can play a role in further declining a currently deteriorated pipe.

Typically, there is less rainfall during the summer, causing the soil to be dry and therefore remain very loose. This allows the pipes to shift and/or expand, which can lead to pipe bursts and leakage as a result. Additionally, hot and dry weather calls for more showers, frequent recreational use of water in general, frequent watering of lawns and plants, and more drinking water consumption. These factors can create a higher-than-normal water demand, which results in an increased pressure on the WDN. If the pipes are not in a good condition, are aging or rusting, an increase in water demand can lead to a leak in the pipeline, or worse, they may burst causing a complete failure. Moreover, if a pipe is clogged, the water pressure can increase to an extent that can lead to cracking and leakage. Additionally, temperature changes in winter can cause the pipes to contract on cooling causing cracks and leaks as a result. Furthermore, in this season typically water consumption is reduced, causing a rise in the water pipe pressure which may lead to leaks. Additionally, any change in soil characteristics due to extreme weather fluctuations can affect the pipeline infrastructure, which may cause the imbalance between WDN sections and fittings, and trigger pipe wall rupture, water leakage, as well as pipe bursts [60].In seasonal transitions, such as the month of October, the water consumption and weather conditions are typically less extreme and hence, the pressure on the pipes is typically low. Another perspective to consider is the time factor between the experiments. Pipes that had been damaged during the month of October (due to aging, temperature change, or construction anomalies) could continue to deteriorate over the course of the year if mitigative measures are not taken to fix/replace them [61].

The results obtained in this study suggest that the proposed method is robust and efficient for leak detection in WDNs. Additionally, the automated model provides means for near real-time processing, which is an added benefit to the detection process, which would enable for timely response for corrective maintenance, while minimizing future risk, understanding the network's behavior, identifying the frequent areas of leaks/bursts, and simultaneously saving water, time, and efforts [62]. Moreover, the visual display of the different data layers and the results of the model in GIS overlaid with the WDN, the map of the city, and the road network, would help in providing sufficient information when deploying a drone with an IR camera and a navigation system over the suspected leak locations. It can also provide an understanding of the network behavior and critical zones identification for optimal management and operation of the WDN. Furthermore, the method utilizes existing pipe sensors which can eliminate the cost associated with other means of leakage detection. The method also proved its applicability on a large-scale network.

The processed IR images were able to robustly detect leaks in the pilot WDN. The detection method was not affected by the pipe material or thickness. In addition, the leak location identification, by assigning a specified number of pixels, allowed for minimal user intervention during the phase of image processing. In addition to its low computational complexity, this method allowed for swift analysis especially when the image load is high. The employed multitemporal IR technique was able to eliminate noise as well. Although, in some cases this method could fail to fully eliminate shadows. One proposed solution for this issue is to obtain a temporal variation image (TVI) where shadow temperatures would remain constant when the leak temperature varies. This method was proven successful in distinguishing leaky from non-leaky areas characterized by low temperatures [58].

Chapter 6. Conclusion and Future Work

Leakage in WDNs is a major concern for water utility companies. Hence, a timely inspection of the network is required for early detection of fluctuations in the system that are indicative of leaks. This arises the necessity of exploring the possible approaches to remedy the issue. In this study, a smart leak detection method was developed using GIS and remote sensing techniques. The method utilizes data from the pressure, flow and water quality monitoring sensors installed within WDNs to detect irregularities that occur within the system in real time. The proposed method was tested using a portion of Sharjah's WDN. This method starts by identifying potential leak areas in GIS by combing pressure, flow and chlorine measurements in the WDN. Subsequently, a drone equipped with an IR camera and a navigation system was to be deployed to these areas to pinpoint the leak coordinates. However, due to the pandemic, a lab setup was prepared instead to mimic a leak in a WDN to manually capture the IR images required for the process. Results of the system validation indicated the effectiveness of proposed method in detecting and locating leaks in WDNs.

This study, having addressed the drawbacks of the leak detection methods currently in use, proposed a leak detection system that is capable of:

- Real time leak detection, saving significant resources for the water utility companies.
- Timely corrective maintenance of WDNs.
- The method utilizes existing monitoring sensors in WDNs, which can eliminate the cost associated with other means of leakage detection.
- Proved its applicability on a real-scale network.
- Having the system to be developed for use by a drone equipped with an IR camera and a navigation system would allow for automated image georeferencing and processing to identify the leak locations with the help of the GIS customized interface.
- The proposed system is novel for leak identification.

As for future work, a drone equipped with a hyperspectral IR camera and a navigation system will be employed to automate the full process on Sharjah WDN. Having the system to be drone-based equipped with an IR camera coupled with GPS would allow for geo-referencing the images, as well as provide real time image loading and processing. The images would automatically be processed to identify moist spots on the ground. This integrated with the customized GIS interface will allow for timely leak detection.

References

[1] A. Ako Ako, J. Shimada, G. E. T. Eyong, and W. Y. Fantong, "Access to potable water and sanitation in Cameroon within the context of Millennium Development Goals (MDGS)," *Water Sci. Technol.*, vol. 61, no. 5, pp. 1317–1339, 2010, doi: 10.2166/wst.2010.836.

[2] T. Oki and K. Shinjiro, "Global Hydrological Cycles and World Water Resources," *Science (80-.).*, vol. 313, no. 5790, pp. 1068–1073, 2006.

[3] O. Hunaidi and W. T. Chu, "Acoustical characteristics of leak signals in plastic water distribution pipes," *Appl. Acoust.*, vol. 58, no. 3, pp. 235–254, 1999, doi: 10.1016/S0003-682X(99)00013-4.

[4] A. Awwad, M. Yahyia, L. Albasha, M. M. Mortula, and T. Ali, "Communication Network for Ultrasonic Acoustic Water Leakage Detectors," *IEEE Access*, vol. 8, pp. 29954–29964, 2020, doi: 10.1109/ACCESS.2020.2972648.

[5] A. Awwad, M. Yahya, L. Albasha, M. M. Mortula, and T. Ali, "Remote thermal water leakage sensor with a laser communication system," *IEEE Access*, vol. 8, pp. 163784–163796, 2020, doi: 10.1109/ACCESS.2020.3022213.

[6] D. Chatzigeorgiou, K. Youcef-Toumi, and R. Ben-Mansour, "Design of a novel in-pipe reliable leak detector," *IEEE/ASME Trans. Mechatronics*, vol. 20, no. 2, pp. 824–833, 2015, doi: 10.1109/TMECH.2014.2308145.

[7] Y. Kim, S. J. Lee, T. Park, G. Lee, J. C. Suh, and J. M. Lee, "Robust leak detection and its localization using interval estimation for water distribution network," *Comput. Chem. Eng.*, vol. 92, pp. 1–17, 2016, doi: 10.1016/j.compchemeng.2016.04.027.

[8] R. Pérez, V. Puig, J. Pascual, A. Peralta, E. Landeros, and L. Jordanas, "Pressure sensor distribution for leak detection in Barcelona water distribution network," *Water Sci. Technol. Water Supply*, vol. 9, no. 6, pp. 715–721, 2009, doi: 10.2166/ws.2009.372.

[9] A. Atef, T. Zayed, A. Hawari, M. Khader, and O. Moselhi, "Automation in

Construction Multi-tier method using infrared photography and GPR to detect and locate water leaks," *Autom. Constr.*, vol. 61, pp. 162–170, 2016, doi: 10.1016/j.autcon.2015.10.006.

[10] H. Aslam, M. Kaur, S. Sasi, M. M. Mortula, S. Yehia, and T. Ali, "Detection of Leaks in Water Distribution System using Non-Destructive Techniques," in *IOP Conference Series: Earth and Environmental Science*, 2018, vol. 150, no. 1, doi: 10.1088/1755-1315/150/1/012004.

[11] J. Yang, Y. Wen, and P. Li, "Leak acoustic detection in water distribution pipelines," *Proc. World Congr. Intell. Control Autom.*, pp. 3057–3061, 2008, doi: 10.1109/WCICA.2008.4594487.

[12] M. Ahadi and M. S. Bakhtiar, "Leak detection in water-filled plastic pipes through the application of tuned wavelet transforms to Acoustic Emission signals," *Appl. Acoust.*, vol. 71, no. 7, pp. 634–639, 2010, doi: 10.1016/j.apacoust.2010.02.006.

[13] Y. Gao, M. J. Brennan, P. F. Joseph, J. M. Muggleton, and O. Hunaidi, "On the selection of acoustic/vibration sensors for leak detection in plastic water pipes," *J. Sound Vib.*, vol. 283, no. 3–5, pp. 927–941, 2005, doi: 10.1016/j.jsv.2004.05.004.

[14] J. Mashford, D. De Silva, D. Marney, and S. Burn, "An approach to leak detection in pipe networks using analysis of monitored pressure values by support vector machine," in *NSS 2009 - Network and System Security*, 2009, pp. 534–539, doi: 10.1109/NSS.2009.38.

[15] Z. Y. Wu, P. Sage, and D. Turtle, "Pressure-dependent leak detection model and its application to a district water system," *J. Water Resour. Plan. Manag.*, vol. 136, no. 1, pp. 116–128, 2010, doi: 10.1061/(ASCE)0733-9496(2010)136:1(116).

[16] M. V. Casillas, L. E. Garza-Castanon, and V. Puig, "Extended-horizon analysis of pressure sensitivities for leak detection in water distribution networks: Application to the Barcelona network," in *2013 European Control Conference, ECC 2013*, 2013, no. 1, pp. 404–409, doi: 10.23919/ecc.2013.6669568.

[17] S. E. Christodoulou, A. Gagatsis, S. Xanthos, S. Kranioti, A. Agathokleous, and M. Fragiadakis, “Entropy-Based Sensor Placement Optimization for Waterloss Detection in Water Distribution Networks,” *Water Resour. Manag.*, vol. 27, no. 13, pp. 4443–4468, 2013, doi: 10.1007/s11269-013-0419-8.

[18] D. Sala and P. Kołakowski, “Detection of leaks in a small-scale water distribution network based on pressure data - Experimental verification,” *Procedia Eng.*, vol. 70, pp. 1460–1469, 2014, doi: 10.1016/j.proeng.2014.02.161.

[19] Y. Ishido and S. Takahashi, “A new indicator for real-time leak detection in water distribution networks: Design and simulation validation,” *Procedia Eng.*, vol. 89, pp. 411–417, 2014, doi: 10.1016/j.proeng.2014.11.206.

[20] R. Sarrate, J. Blesa, F. Nejjari, and J. Quevedo, “Sensor placement for leak detection and location in water distribution networks,” *Water Sci. Technol. Water Supply*, vol. 14, no. 5, pp. 795–803, 2014, doi: 10.2166/ws.2014.037.

[21] M. V. Casillas, L. E. Garza-Castañón, and V. Puig, “Optimal sensor placement for leak location in water distribution networks using evolutionary algorithms,” *Water (Switzerland)*, vol. 7, no. 11, pp. 6496–6515, 2015, doi: 10.3390/w7116496.

[22] M. Cugueró-Escofet, V. Puig, and J. Quevedo, “Optimal pressure sensor placement and assessment for leak location using a relaxed isolation index: Application to the Barcelona water network,” *Control Eng. Pract.*, vol. 63, no. September, pp. 1–12, 2017, doi: 10.1016/j.conengprac.2017.03.003.

[23] A. Soldevila, J. Blesa, S. Tornil-Sin, R. M. Fernandez-Canti, and V. Puig, “Sensor placement for classifier-based leak localization in water distribution networks using hybrid feature selection,” *Comput. Chem. Eng.*, vol. 108, pp. 152–162, 2018, doi: 10.1016/j.compchemeng.2017.09.002.

[24] J. Saldarriaga and C. A. Salcedo, “Determination of optimal location and settings of pressure reducing valves in water distribution networks for minimizing water losses,” *Procedia Eng.*, vol. 119, no. 1, pp. 973–983, 2015, doi: 10.1016/j.proeng.2015.08.986.

[25] A. M. Sadeghioon, N. Metje, D. N. Chapman, and C. J. Anthony, “SmartPipes: Smart wireless sensor networks for leak detection in water pipelines,” *J. Sens. Actuator Networks*, vol. 3, no. 1, pp. 64–78, 2014, doi: 10.3390/jsan3010064.

[26] M. Mulholland, A. Purdon, M. A. Latifi, C. Brouckaert, and C. Buckley, “Leak identification in a water distribution network using sparse flow measurements,” *Comput. Chem. Eng.*, vol. 66, pp. 252–258, 2014, doi: 10.1016/j.compchemeng.2013.11.017.

[27] E. Farah and I. Shahrour, “Leakage Detection Using Smart Water System: Combination of Water Balance and Automated Minimum Night Flow,” *Water Resour. Manag.*, vol. 31, no. 15, pp. 4821–4833, 2017, doi: 10.1007/s11269-017-1780-9.

[28] T. AL-Washali, S. Sharma, F. AL-Nozaily, M. Haidera, and M. Kennedy, “Modelling the leakage rate and reduction using minimum night flow analysis in an intermittent supply system,” *Water (Switzerland)*, vol. 11, no. 1, 2018, doi: 10.3390/w11010048.

[29] J. Jiménez-Cabas, E. Romero-Fandiño, L. Torres, M. Sanjuan, and F. R. López-Estrada, “Localization of Leaks in Water Distribution Networks using Flow Readings,” *IFAC-PapersOnLine*, vol. 51, no. 24, pp. 922–928, 2018, doi: 10.1016/j.ifacol.2018.09.685.

[30] A. Pal and K. Kant, “Water flow driven sensor networks for leakage and contamination monitoring in distribution pipelines,” *ACM Trans. Sens. Networks*, vol. 15, no. 4, 2019, doi: 10.1145/3342513.

[31] C. Fan, F. Sun, and L. Yang, “Investigation on nondestructive evaluation of pipelines using infrared thermography,” in *The Joint 30th International Conference on Infrared and Millimeter Waves and 13th International Conference on Terahertz Electronics, 2005. IRMMW-THz 2005.*, 2005, vol. 2, pp. 339–340, doi: 10.1109/icimw.2005.1572551.

[32] P. M. Bach and J. K. Kodikara, “Reliability of Infrared Thermography in Detecting Leaks in Buried Water Reticulation Pipes,” *IEEE J. Sel. Top. Appl. Earth Obs. Remote Sens.*, vol. 10, no. 9, pp. 4210–4224, 2017, doi:

10.1109/JSTARS.2017.2708817.

[33] M. Fahmy, P. Eng, A. M. Asce, O. Moselhi, P. Eng, and F. Asce, “Automated Detection and Location of Leaks in Water Mains Using Infrared Photography,” vol. 24, no. June, pp. 242–248, 2010, doi: 10.1061/(ASCE)CF.1943-5509.0000094.

[34] L. Resolution, I. Cameras, F. Evaluating, and D. R. Detection, “Detection of Water Leakage in Buried Pipes Using Infrared Technology ;,” 2015.

[35] M. Nakhkash and M. R. Mahmood-Zadeh, “Water leak detection using ground penetrating radar,” in *Proceedings of the Tenth International Conference Ground Penetrating Radar, GPR 2004*, 2004, vol. 2, no. February, pp. 525–528, doi: 10.1109/ICGPR.2004.179793.

[36] S. Hyun, Y. Jo, H. Oh, S. Kim, and Y. Kim, “The laboratory scaled-down model of a ground-penetrating radar for leak detection of water pipes,” vol. 2791, doi: 10.1088/0957-0233/18/9/008.

[37] M. Bimpas, A. Amditis, and N. K. Uzunoglu, “Design and Implementation of an Integrated High Resolution Imaging Ground Penetrating Radar for Water Pipeline Rehabilitation,” *Water Resour. Manag.*, vol. 25, no. 4, pp. 1239–1250, 2011, doi: 10.1007/s11269-010-9631-y.

[38] D. Ayala-Cabrera, M. Herrera, J. Izquierdo, S. J. Ocaña-Levario, and R. Pérez-García, “GPR-based water leak models in water distribution systems,” *Sensors (Switzerland)*, vol. 13, no. 12, pp. 15912–15936, 2013, doi: 10.3390/s131215912.

[39] Hawkeye Services, “Ground Penetrating Radar (GPR).” https://www.hawkeyeservice.com/service/ground-penetrating-radar/ (accessed Nov. 05, 2021).

[40] Government of Canada, “Fundamentals of Remote Sensing - Introduction.” https://www.nrcan.gc.ca/maps-tools-and-publications/satellite-imagery-and-air-photos/tutorial-fundamentals-remote-sensing/introduction/9363 (accessed Nov. 05, 2021).

[41] P. Taylor, A. Agapiou, D. D. Alexakis, K. Themistocleous, and G. Diofantos, “Water leakage detection using remote sensing , field spectroscopy and GIS in semiarid areas of Cyprus,” no. December, pp. 37–41, 2014, doi: 10.1080/1573062X.2014.975726.

[42] J. M. Muggleton, M. J. Brennan, and R. J. Pinnington, “Wavenumber prediction of waves in buried pipes for water leak detection,” *J. Sound Vib.*, vol. 249, no. 5, pp. 939–954, 2003, doi: 10.1006/jsvi.2001.3881.

[43] D. Covas, H. Ramos, and A. Betâmio de Almeida, “Standing wave difference method for leak detection in pipeline systems,” *J. Hydraul. Eng.*, vol. 131, no. 12, pp. 1106–1116, 2005, doi: 10.1061/(ASCE)0733-9429(2005)131:12(1106).

[44] M. Ferrante and B. Brunone, “Pipe system diagnosis and leak detection by unsteady-state tests. 2. Wavelet analysis,” *Adv. Water Resour.*, vol. 26, no. 1, pp. 107–116, 2003, doi: 10.1016/S0309-1708(02)00102-1.

[45] N. I. Sherksi, S. Lias, M. Labeeb, R. Adnan, and M. N. Taib, “Leakage effects on the variables of water distribution system,” in *Proceedings - 2013 IEEE Conference on Systems, Process and Control, ICSPC 2013*, 2013, no. December, pp. 42–45, doi: 10.1109/SPC.2013.6735100.

[46] V. Ghorbanian, B. Karney, and Y. Guo, “Pressure standards in water distribution systems: Reflection on current practice with consideration of some unresolved issues,” *J. Water Resour. Plan. Manag.*, vol. 142, no. 8, p. 04016023, 2016, doi: 10.1061/(ASCE)WR.1943-5452.0000665.

[47] National Research Council, *Drinking water distribution systems: Assessing and reducing risks*. Washington, D.C.: The National Academies Press, 2006.

[48] M. Cugueró-Escofet, V. Puig, J. Quevedo, and J. Blesa, “Optimal pressure sensor placement for leak localisation using a relaxed isolation index: Application to the Barcelona water network,” *IFAC-PapersOnLine*, vol. 28, no. 21, pp. 1108–1113, 2015, doi: 10.1016/j.ifacol.2015.09.675.

[49] W. Zeng *et al.*, “Leak Detection for Pipelines Using In-Pipe Optical Fiber Pressure Sensors and a Paired-IRF Technique,” *J. Hydraul. Eng.*, vol. 146, no.

10, pp. 1–6, 2020, doi: 10.1061/(ASCE)HY.1943-7900.0001812.

[50] M. M. Mortula, T. A. Ali, R. Sadiq, A. E. Idris, and A. Al Mulla, “Impacts of Water Quality on the Spatiotemporal Susceptibility of Water Distribution Systems,” *Clean - Soil, Air, Water*, vol. 47, no. 5, pp. 1–12, 2019, doi: 10.1002/clen.201800247.

[51] R. Łangowski and M. A. Brdys, “An optimised placement of the hard quality sensors for a robust monitoring of the chlorine concentration in drinking water distribution systems,” *J. Process Control*, vol. 68, pp. 52–63, 2018, doi: 10.1016/j.jprocont.2018.04.007.

[52] World Health Organization, “Technical Notes on Drinking Water, Sanitation and Hygiene in Emergencies: Measuring Chlorine Levels in Water Supplies,” 2011. [Online]. Available: www.who.int/water_sanitation_health.

[53] J. P. Delhomme, “Spatial variability and uncertainty in groundwater flow parameters: A geostatistical approach,” *Water Resour. Res.*, vol. 15, no. 2, pp. 269–280, 1979, doi: 10.1029/WR015i002p00269.

[54] A. K. Toubal, M. Achite, S. Ouillon, and A. Dehni, “Soil erodibility mapping using the RUSLE model to prioritize erosion control in the Wadi Sahouat basin, North-West of Algeria,” *Environ. Monit. Assess.*, vol. 190, no. 4, 2018, doi: 10.1007/s10661-018-6580-z.

[55] P. M. Bartier and C. P. Keller, “Multivariate interpolation to incorporate thematic surface data using inverse distance weighting (IDW),” *Comput. Geosci.*, vol. 22, no. 7, pp. 795–799, 1996, doi: 10.1016/0098-3004(96)00021-0.

[56] F. Huang, D. Liu, X. Tan, J. Wang, Y. Chen, and B. He, “Explorations of the implementation of a parallel IDW interpolation algorithm in a Linux cluster-based parallel GIS,” *Comput. Geosci.*, vol. 37, no. 4, pp. 426–434, 2011, doi: 10.1016/j.cageo.2010.05.024.

[57] K. Zhao, Q. Qi, A. Zhang, L. Jiang, and Q. Liang, “The influence of planting angle on maize based on GIS,” in *2016 5th International Conference on Agro-*

Geoinformatics, Agro-Geoinformatics 2016, 2016, p. 5, doi: 10.1109/Agro-Geoinformatics.2016.7577609.

[58] M. Yahia, R. Gawai, T. Ali, M. M. Mortula, L. Albasha, and T. Landolsi, "Non-Destructive Water Leak Detection Using Multitemporal Infrared Thermography," *IEEE Access*, vol. 9, pp. 72556–72567, 2021, doi: 10.1109/ACCESS.2021.3078415.

[59] W. Di, S. Li, and X. Liang, "Analysis of Chinese media reports on water pipe burst events in 2010," *Appl. Mech. Mater.*, vol. 316–317, pp. 727–731, 2013, doi: 10.4028/www.scientific.net/AMM.316-317.727.

[60] B. A. Wols and P. Van Thienen, "Impact of weather conditions on pipe failure: A statistical analysis," *J. Water Supply Res. Technol. - AQUA*, vol. 63, no. 3, pp. 212–223, 2014, doi: 10.2166/aqua.2013.088.

[61] L. Huang, S. Li, Y. Hou, W. Zhou, and J. Zou, "Statistical analysis of domestic web news reported burst events on municipal water distribution system in 2011," *Appl. Mech. Mater.*, vol. 212–213, pp. 619–627, 2012, doi: 10.4028/www.scientific.net/AMM.212-213.619.

[62] A. Ayad, A. Khalifa, and M. Fawy, "A Model-Based Approach for Leak Detection in Water Distribution Networks Based on Optimisation and GIS Applications," *Civ. Environ. Eng.*, vol. 17, no. 1, pp. 277–285, 2021, doi: 10.2478/cee-2021-0029.

[63] MTA Service, "Leak Detection." http://mta-service.eu/leak_detection.php?l=en (accessed Nov. 15, 2021).

Vita

Doha Elshazly was born in 1997, in Tokyo, Japan. She received her primary and secondary education in Dubai, UAE. She received her B.Sc. degree in Civil and Environment Engineering from the University of Sharjah in 2018. From 2018 to 2019, she worked as a Research and Development Engineer in the university.

In September 2019, she joined the Civil Engineering master's program in the American University of Sharjah while simultaneously working as a graduate teaching assistant. Due to her exceptional academic scores, she was elected the valedictorian of the class of spring 2021.